Palmitoylated Cysteines in Chikungunya Virus nsP1 Are Critical for Targeting to Cholesterol-Rich Plasma Membrane Microdomains with Functional Consequences for Viral Genome Replication

William Bakhache, Aymeric Neyret, Eric Bernard, Andres Merits, Laurence Briant

Palmitoylated cysteines in Chikungunya virus nsP1 are critical for targeting to cholesterol-rich plasma membrane microdomains with functional consequences for viral genome replication

William Bakhache [a], Aymeric Neyret [a], Eric Bernard [a], Andres Merits [b] and Laurence Briant [a#]

[a] IRIM, Univ. Montpellier - CNRS UMR9004, Montpellier, France.

[b] Institute of Technology, University of Tartu, Tartu, Estonia.

Running head: CHIKV nsP1 affinity for cholesterol enriched membranes

[#] Address correspondence to Laurence Briant, IRIM - Institut de recherche en Infectiologie de Montpellier, UMR9004 CNRS-UM. 1919 route de Mende 34293 Montpellier Cedex 5 laurence.briant@irim.cnrs.fr

Key words: Chikungunya virus, Methyl/guanylyltransferase, Cholesterol, Plasma membrane, Replication complexes, Alphavirus,

Abstract

In mammalian cells, alphavirus replication complexes are anchored to the plasma membrane. This interaction with lipid bilayers is mediated through the viral methyl/guanylyltransferase nsP1 and reinforced by palmitoylation of cysteine residue(s) in the C-terminal region of this protein. Lipid content of membranes supporting nsP1 anchoring remains poorly studied. Here, we explore the membrane binding capacity of nsP1 with regards to cholesterol. Using the medically important Chikungunya virus (CHIKV) as a model, we report that nsP1 co-segregates with cholesterol-rich detergent-resistant membrane microdomains (DRMs), also called lipid rafts. In search for critical factor for cholesterol partitioning, we identify nsP1 palmitoylated cysteines as major players in this process. In cells infected with CHIKV or transfected with CHIKV trans-replicase plasmids, nsP1, together with the other nonstructural proteins, are detected in DRMs. While the functional importance of CHIKV nsP1 preference for cholesterol-rich membrane domains remains to be determined, we observed that U18666A- and imipramine-induced sequestration of cholesterol in late endosomes redirected nsP1 to these compartments and simultaneously dramatically decreased CHIKV genome replication. A parallel study of Sindbis virus (SINV) revealed that nsP1 from this divergent alphavirus displays a low affinity for cholesterol and only moderately segregates with DRMs. Behaviors of CHIKV and SINV with regards to cholesterol therefore match with the previously reported differences in requirement for nsP1 palmitoylation, that is dispensable for SINV but strictly required for CHIKV replication. Altogether, this study highlights the functional importance of nsP1 segregation with DRMs and provides new insight into the functional role of nsP1 palmitoylated cysteines during alphavirus replication.

Importance

Functional alphavirus replication complexes are anchored to the host cell membranes through the interaction of nsP1 with the lipid bilayers. In this work, we investigate the importance of cholesterol

for such association. We show that nsP1 has affinity for cholesterol-rich membrane microdomains formed at the plasma membrane and identify conserved palmitoylated cysteine(s) in nsP1 as the key determinant for cholesterol affinity. We demonstrate that drug-induced cholesterol sequestration in late endosomes not only redirects nsP1 to this compartment but also dramatically decreases genome replication, suggesting the functional importance of nsP1 targeting to cholesterol-rich plasma membrane microdomains. Finally, we evidence that nsP1 from Chikungunya and Sindbis viruses display different sensitivity to cholesterol sequestering agents, that parallel with their difference in the requirement for nsP1 palmitoylation for replication. This research, therefore, gives new insight into the functional role of palmitoylated cysteines in nsP1 for the assembly of functional alphavirus replication complexes in their mammalian host.

Introduction

In the last decade, evidence has pointed toward the intricate relationship between host lipid metabolism and the replication of viral pathogens. Indeed, viruses can co-opt or reprogram lipid signaling, synthesis and metabolism either to generate ATP, to extend cellular membranes or to remodel membrane lipid content. These modifications will serve to create an environment that is optimal for viral replication. This need is dictated by the pivotal role played by membranes in almost all steps of the virus life cycle. Indeed, the importance of cellular lipids during the binding/entry process and assembly/budding of new infectious progeny into the extracellular space has long been appreciated (for review see (1)). However, the discovery that viruses with a positive-strand RNA genome ((+)RNA viruses) replicate in association with host cell membranes has expanded the regulatory function of lipids to genome replication. It is now well established that such viruses create membranous compartments, also called virus replication organelles, originating from the endoplasmic reticulum (ER), Golgi apparatus, mitochondria, peroxisomes, endosomes/lysosomes or from the plasma membrane (PM) (2). In these compartments, viral replication proteins bind cell membranes with an affinity for determined lipid species (3, 4).

Cell membranes are composed of phospholipids, glycolipids, and cholesterol. Among other lipids, cholesterol constitutes a unique type of cellular membrane building block. It is responsible for regulating fluidity and impermeability to lipid bilayers. In vertebrate cells, cholesterol homeostasis is maintained through *de novo* synthesis in the ER, with 3-hydroxy-3-methylglutaryl-coenzyme A (HMG-CoA) reductase being the rate-limiting enzyme, and through receptor-mediated intake from the extracellular medium in the form of low-density lipoproteins (LDLs) (5). In this scenario, LDLs are delivered to and hydrolyzed in late endosomes/lysosomes (LE/Ls) where free cholesterol is released. Then, cholesterol requires proper intracellular transport to exit the LE/Ls and reach its final destination mainly at the PM, in the Golgi apparatus and the ER. This is ensured by Niemann-Pick C 1 and 2 (NPC1 and NPC2) proteins localized at the limiting membrane of lysosomes and in the

79 lysosomal lumen respectively (6). Once at the PM, cholesterol together with glycosphingolipids,
80 glycophosphatidylinositol (GPI)-anchored proteins and transmembrane proteins can cluster into
81 discrete domains. These cholesterol-enriched detergent-resistant membrane microdomains, referred
82 to as DRMs or lipid rafts, have been identified as platforms for both endocytosis of penetrating viral
83 particles and for progeny assembly and budding (7). More recently, cholesterol regulatory function
84 was extended to the replication step of (+)RNA viruses. The local accumulation of cholesterol was
85 proposed to contribute to the creation of a membrane microenvironment conducive to assembly and
86 optimal functionning of replication complexes formed by members of the *Flaviviridae* family,
87 including hepatitis C virus (HCV) (8–10) and West Nile virus (11), by members of *Picornaviridae*
88 family, including Coxsackievirus and poliovirus (12) and by plant viruses from the *Bromoviridae* family
89 (Brome mosaic virus; BMV) (13). Consistent with the idea that cholesterol accumulation may be
90 required for optimal activity of viral replication machinery, manipulation of cholesterol metabolism
91 was found to impair genome replication of taxonomically divergent (+)RNA viruses (8, 12, 14–18).

92 Alphaviruses are (+)RNA viruses, which are predominantly transmitted to vertebrates by mosquito
93 vectors. Chikungunya virus (CHIKV) is an Old World alphavirus causing millions of infections in
94 tropical and subtropical geographical areas with a potential risk of spreading to regions with a
95 temperate climate. It has recently received significant attention as a consequence of its re-
96 emergence in the Indian Ocean and Caribbean Islands before spreading worldwide (19). CHIKV, like
97 other alphaviruses, replicates its genome in membranous niches derived from the host PM (20–22).
98 The replication complex confined in these organelles, termed as spherules, contains the four non-
99 structural proteins nsP1, nsP2, nsP3 and nsP4 encoded by the 5' ORF in the viral genome which are
100 expressed in the form of P123 and P1234 polyprotein precursors. In this complex, membrane binding
101 is mediated by nsP1, the viral methyltransferase (MTase) and guanylyltransferase (GTase), which
102 catalyzes the formation of the cap structure at the 5' end of nascent positive stand viral RNAs (23,
103 24). A putative α-helix central to nsP1 was proposed to play a crucial role for membrane attachment
104 (25, 26). S-acylated cysteines located in the C-terminal region of this protein were then proposed to

stabilize this interaction (27). The functional requirement for nsP1 interaction with membranes varies among alphaviruses. It is strictly required for Semliki Forest virus (SFV) nsP1 enzymatic activity (28) while it is dispensable for that of Sindbis virus (SINV) nsP1 (29). More specifically, alanine substitution of palmitoylated cysteines has only a marginal inhibitory effect on SINV replication (30, 31) while leading to the acquisition of compensatory mutations for SFV (31, 32). Recently, this mutation was reported to completely abolish the replication of CHIKV (33, 34).

In vitro, SFV nsP1 has affinity for anionic phospholipids especially phosphatidylserine, phosphatidylglycerol, and cardiolipin; these lipid species significantly improve its capping activity (25, 28). In cells, however, nsP1 affinity for specific lipids remains almost uninvestigated. In recent years, cholesterol metabolism was reported to be critical for the replication of alphavirus genome. Indeed, SINV RNA replication and protein synthesis is significantly decreased in fibroblasts from patients with type A Niemann-Pick disease (NPD-A) which induces cholesterol and sphingolipid storage in LE/Ls (35). More recently, we reported that U18666A, a class II cationic amphipathic steroid 3-β-[2-(diethylamine)ethoxy]androst-5-en-17-one, and the anti-depressant drug imipramine, which both phenocopy NPD-A, are CHIKV inhibitors with potential activity against RNA replication steps (16). Here, we further question the importance of cholesterol metabolism in the alphavirus life cycle. We especially explore the outcome of cholesterol manipulation on nsP1 subcellular distribution and membrane anchoring. We show that nsP1 has affinity for cholesterol-rich membranes. Indeed, U18666A or imipramine redirect CHIKV nsP1 to Lamp2-positive endosomes where unesterified cholesterol accumulates. At the plasma membrane, nsP1 co-segregates with cholesterol-containing DRMs as attested by membrane flotation assays. Investigating the molecular basis of nsP1 targeting to DRMs revealed that the cysteines, previously reported to be palmitoylated (34), are the main determinants for association with these domains. Interestingly, when expressed transiently in the context of a P1234 polyprotein precursor or by an infectious CHIKV, nsP2, nsP3, and nsP4 were found to co-segregate with nsP1 in cholesterol-rich membrane fractions, a property that was abolished when nsP1 cysteines were mutated. In a parallel study we found that cysteine-mediated nsP1

association with cholesterol-rich membranes is conserved for SINV despite being less marked than for CHIKV. Moreover, SINV nsP1 was also less sensitive to U18666A-induced cholesterol sequestration. This phenotype with regard to nsP1 cholesterol partitioning parallels the reduced requirement for cysteine palmitoylation previously reported for SINV replication (30, 31). Altogether this study provides clues on the proviral role of cholesterol in alphavirus replication, suggesting its regulatory function in nsPs association with the PM and presumably in the formation of functional replication complexes.

Results

Cholesterol is pivotal for alphavirus genome replication.

First, we set out to study the involvement of cholesterol homeostasis in CHIKV replication. Cholesterogenesis was inhibited using lovastatin, an FDA-approved inhibitor of HMG-CoA reductase, that catalyzes the conversion of HMG-CoA to mevalonate in the cholesterol biosynthesis pathway (Fig 1A) (36). Cholesterol availability at the PM was reduced using U18666A or imipramine. By targeting NPC1 transporter, both drugs block the transfer of endocytosed cholesterol from late endosomes to different organelles, including the PM, without significant effect on other lipid species (37). Additionally, U18666A inhibits enzymes of the cholesterol synthesis pathway (38). Each drug, used in a concentration range that was controlled to have limited toxicity (Fig 1B-b,d,f), was added to HEK293T cells 30 mins before infection with CHIKV-LR-5'GFP at a multiplicity of infection (MOI) of 0.5. Cells were maintained in culture with the drugs for 24 hrs and then infection was monitored measuring levels of GFP reporter expressed by this recombinant virus. In each case, CHIKV infection was significantly reduced as compared with the mock-treated condition (Fig 1B-a,c,e).

We and others have demonstrated that the depletion of membrane cholesterol is deleterious for fusion of the virion and host membranes (39, 40). Because host membranes are also pivotal for replication of alphavirus genome through the creation of membranous replication organelles, we

155 investigated whether cholesterol biosynthesis is also required for the post-entry step of CHIKV
156 infection cycle. To this end, we performed experiments in which cells were treated with cholesterol
157 metabolism and transport inhibitors 1 hr after CHIKV infection. In these conditions, lovastatin,
158 U18666A and imipramine decreased CHIKV genome replication (Fig 2A). To definitively omit drug
159 effects on viral entry, we finally took advantage of a CHIKV trans-replication system that
160 recapitulates post-entry events of CHIKV life cycle (33). Plasmids CMV-P1234 and HSPolI-Fluc-Gluc,
161 encoding the P1234 polyprotein and a replication-competent template RNA containing firefly and
162 *Gaussia* luciferase reporter genes under the control of genomic and subgenomic viral promoters
163 respectively (Fig 2B), were cotransfected in HEK293T cells. Consequences of cholesterol transport
164 inhibition were assayed by adding increasing concentrations of lovastatin, U18666A, and imipramine
165 to transfected cells and quantification of reporter activities in cell lysates. As depicted in Figure 2C,
166 reporter expression directed by both genomic and subgenomic promoters was decreased by the
167 drugs when compared to control conditions. Altogether, these results indicate that cholesterol
168 homeostasis, including ongoing biosynthesis and transport of unesterified cholesterol to the host
169 membranes, is pivotal for CHIKV genome replication.

170 **α-helix and putative palmitoylated cysteines cooperate for CHIKV nsP1 binding to host**
171 **membranes.**

172 Alphavirus replication complexes are anchored to the host membranes thanks to nsP1 membrane
173 binding capacity. While extensively reported for nsP1 encoded by SFV and SINV (25, 30), this feature
174 has not yet been studied functionally for CHIKV. To investigate CHIKV nsP1 behavior with regard to
175 host cell membranes, a plasmid encoding a GFP-fused CHIKV nsP1 protein (GFP-nsP1; Fig 3A) was
176 generated and used to transfect HEK293T cells. NsP1 membrane association was investigated by
177 fractionation of transfected cells. Post-nuclear extract prepared from GFP-nsP1-expressing cells was
178 separated into membranous (P25) and cytosolic (S25) samples by differential centrifugation as
179 previously reported (41). Each fraction was resolved using SDS-PAGE and probed with anti-GFP

antibodies and with antibodies against Na^+/K^+ ATPase or GAPDH, that respectively associate with membrane and cytosolic compartments. In these conditions, GFP alone was detected in the cytosolic sample together with GAPDH (Fig 3B and 3C). By contrast, GFP-nsP1 was detected in the membrane fraction also containing Na^+/K^+ ATPase. In parallel HeLa cells expressing these proteins were analyzed using confocal microscopy. As expected, the fluorescence of individual GFP was diffuse in the cytoplasm and nucleus. However, GFP-nsP1 fluorescence overlapped with PM stained using wheat germ hemagglutinin (WGA)-conjugated with Alexa Fluor 647 (Fig 3D). As previously reported for related alphaviruses (42), expression of GFP-nsP1 generated huge membrane reshaping creating filopodia- and lamellipodia-like structures covering the entire cell surface, that stained positive for the green fluorescence. Of note, this profile was also observed for a C-terminally GFP-tagged nsP1-GFP protein as well as for an untagged nsP1 detected by mean of anti-nsP1 serum (Fig 3E), thereby supporting that GFP-nsP1 behaves as native nsP1 regarding localization and association with membranes. According to the focal plane chosen, a fraction of each of these proteins was also detected as small cytosolic aggregates as illustrated in Figure 3E.

Because alphavirus nsP1 was previously proposed to be trafficked to endosomes (43) and in light of our confocal microscopy analysis, we further questioned nsP1 subcellular distribution by performing fractionation assays that separated the PM from other cell membranes. The post-nuclear extract was prepared from GFP-nsP1 expressing cells and separated by isopycnic centrifugation in a self-forming linear 10-20-30% iodixanol density gradient. Twenty-four samples were collected from top to bottom and assayed by western blotting for GFP-nsP1 content. A roughly equal proportion of GFP-nsP1 was detected in the top fractions 1 and 2 and also in fractions 9 to 12 that all stained positive for the Na^+/K^+ ATPase membrane marker (Fig 3F). These fractions also contained flotillin-1 (FLOT1) that is known to localize predominantly to the PM and endosomal compartments, *i.e.* late endosomes and recycling endosomes (44). By contrast, individual GFP segregated with fractions 17 to 24 at the bottom of the gradient that corresponded to the cytosolic compartment. Altogether, these results show that CHIKV nsP1 is a membrane-associated protein, that cofractionates equally with the PM

and some internal membranes, probably endosomal in nature, suggesting that this protein may traffic between the two compartments.

We next questioned whether the functions of membrane binding determinants previously identified in alphavirus nsP1 proteins are also conserved for CHIKV nsP1. Extensive analysis performed using SFV and SINV as models established that membrane association of nsP1 relies on a central conserved sequence that folds as an amphipathic α-helix when studied as a synthetic peptide in solution (25). In this sequence, a pivotal role in membrane anchoring was attributed to tryptophan at position 259 (W_{259}) that sinks into the phospholipid bilayer (25). This interaction was proposed to be reinforced by the presence of cysteine residue at position 420 (C420) in SINV or cysteine residues 418-420 in SFV (C418-420) which are covalently palmitoylated and render the protein highly hydrophobic (27, 30). These motifs are conserved in the CHIKV nsP1 sequence where W258 and C417-419 of residues correspond to W259 and C418-420 of SFV nsP1, respectively (Fig 3A). Recently, C417-419 in CHIKV nsP1 were reported to be palmitoylated (34), therefore further attesting that nsP1 palmitoylation is a conserved feature among Old World alphaviruses. To study the contribution of each motif in CHIKV nsP1 membrane binding, we generated GFP-nsP1 mutants in which W258 (GFP-nsP1$_{W258A}$) or $C_{417-419}$ (GFP-nsP1$_{3A}$) residues in nsP1 sequence were replaced by alanine as well as a double nsP1 mutant bearing a combination of W_{258}A or $C_{417-419}$A mutations (GFP-nsP1$_{DM}$). Fluorescence microscopy of cells transfected with the corresponding plasmids evidenced a diffuse green fluorescence that predominated in the cytoplasm by contrast with cells expressing GFP-nsP1 that was mainly detected at the plasma membrane (Fig 3D). Fractionation experiments confirmed that GFP-nsP1$_{W258A}$ and GFP-nsP1$_{3A}$ were more abundant in the cytosolic fraction than GFP-nsP1, with a significant amount of each mutant protein remaining associated with cell membranes (Fig 3B and 3C). The same cell extracts were then subjected to membrane flotation assay in iodixanol gradient to appreciate their capacity to associate with the internal/plasma membrane compartments. GFP-nsP1$_{W258A}$ and GFP-nsP1$_{3A}$ proteins were both detected in fractions 18-24 of the gradient thereby confirming that these proteins have a decreased membrane affinity (Fig 3F). Each mutant protein was also present at the

top of the gradient in fractions 1-2 corresponding to the PM and in fractions 9-12 corresponding to internal membranes. Distribution of mutant proteins in these fractions generally mimicked that of GFP-nsP1, except that GFP-nsP1$_{W258A}$ was somewhat more abundant in internal membrane fractions. This was also reflected in more diffuse localization of GFP fluorescence in cells expressing GFP-nsP1$_{W258A}$ (compare panels b and d of Fig. 3D) indicating possible role of W258 for PM affinity of CHIKV nsP1. Nevertheless, the observed differences were small suggesting that W_{258}A and $C_{417\text{-}419}$A mutations despite decreasing membrane affinity do not prominently modify nsP1 distribution between intracellular and plasma membranes or nsP1 trafficking capacity. Interestingly, membrane association was further decreased when W_{258}A and $C_{417\text{-}419}$A mutations were combined in GFP-nsP1$_{DM}$ (Fig 3B and 3D). Altogether these results establish that CHIKV nsP1 associates both with the plasma and internal membranes, an association dictated by the cooperation of motifs that contain C417-419 and W258 amino acids in this protein.

Cholesterol storage defect redirects CHIKV nsP1 to late endosomes.

Based on the observation that cholesterol synthesis and transport is required for CHIKV RNA replication and on the intimate relationship of CHIKV nsP1 with membranes, we next wondered whether cholesterol homeostasis has an impact on nsP1 behavior. We first investigated nsP1 subcellular localization with respect to cholesterol distribution. Cells transfected with plasmid expressing GFP-nsP1 were incubated with U18666A or imipramine to generate a cholesterol entrapment in LE/Ls (45). This capacity was controlled using the antifungal antibiotic filipin III that forms a fluorescent complex upon association with unesterified cholesterol (46). In the presence of U18666A or imipramine, filipin III evidenced the formation of large fluorescent cytosolic aggregates that contrasted with the presence of cholesterol at the PM and more evenly distributed in the cytoplasm of mock-treated cells (Fig 4A and data not shown). For U18666A, these clusters colocalized with Lamp2 (Fig 4B), a LE/Ls marker, thereby confirming that this pharmacological agent stimulates the accumulation of unesterified cholesterol in late endosomes as previously reported (47). Using

these experimental conditions, we next assessed the impact of cholesterol storage defect on GFP-nsP1 subcellular localization and membrane affinity. Fractionation assays established that drug treatment did not increase amount of cytosolic nsP1 (Fig 4C; S25 fraction) indicating that it had no consequence on nsP1 membrane affinity. However, microscopy imaging revealed that, in the presence of U18666A, a significant part of GFP-nsP1 fluorescence was redirected from the PM to cytosolic aggregates. This signal overlapped with filipin III staining as attested by cross-sectional analysis of the fluorescent signals (Fig 4D and 4E). In similar experimental conditions, no redistribution of individual GFP fluorescence was observed. Accordingly, upon cholesterol storage condition, GFP-nsP1 colocalized with unesterified cholesterol stored in late endosomes as quantified by calculating Mander's coefficient (Fig 4F). This situation contrasted with that of mock-treated cells in which the GFP-nsP1 fluorescence colocalized with filipin III at the PM and did not overlap with Lamp 2 staining. Altogether, our results argue that the inhibition of NPC1-mediated cholesterol transport by U18666A redirects GFP-nsP1 to LE/Ls where unesterified cholesterol accumulates. Re-targeting GFP-nsP1 to these compartments has no significant impact on nsP1 membrane binding capacity.

C417-419 but not W258 residue determine CHIKV nsP1 sensitivity to cholesterol distribution.

Palmitoylation governs protein trafficking and association with membranes. A major focus of studies on protein palmitoylation has been the role of this modification in promoting interaction with gangliosides and cholesterol, leading at certain conditions, to protein translocation to raft/caveolae membrane domains (48). Given that the C417-429 in CHIKV nsP1 required for optimal membrane association have recently been reported to be palmitoylated (34), we investigated their contribution to GFP-nsP1 cholesterol affinity. The above described experiments were repeated using cells transfected with GFP-nsP1$_{3A}$ plasmid. In the presence of U18666A, GFP-nsP1$_{3A}$ fluorescence remained diffuse in the cytoplasm whether the cells were maintained in the presence of U18666A or with an appropriate concentration of vehicle (Fig 5C). GFP-nsP1$_{W258A}$ fluorescence was concentrated

in cytosolic foci colocalized with filipin III fluorescence (Fig 5A) as observed for GFP-nsP1. These phenotypes were confirmed by cross-sectional analysis of the fluorescent signals (Fig 5B and D) and by calculation of Mander's coefficients (Fig 5E). Accordingly, W258, even if required for strengthening nsP1 membrane affinity, is not critical for cholesterol affinity. In contrast, cysteine-to-alanine substitution in mutant GFP- $nsP1_{3A}$ abolished sensitivity to U18666A, suggesting a critical role of palmitoylated cysteines in nsP1 cholesterol affinity.

To further explore GFP-$nsP1_{3A}$ behavior with regard to cholesterol, we took advantage of CD81, a heavily palmitoylated tetraspanin, segregating mainly with DRMs, as a lipid raft biomarker (49). Indeed, in our hands, this protein was mainly detected at the PM of untreated U2OS cells (Fig 6A). It was redirected to cytosolic aggregates in cells cultured with U18666A or imipramine (Fig 6B) where it colocalized with GFP-nsP1 as attested by Mander's and Pearson's coefficient calculation (Fig 6D and 6E). CD81 therefore appears as a sensitive cholesterol sensor. Using this property, we explored the importance of nsP1 palmitoylated cysteines for cholesterol dependency. Cells transfected to express GFP-$nsP1_{3A}$ were incubated in the presence of U18666A. Despite inducing the clustering of CD81 into intracellular compartments, this treatment did not affect GFP-$nsP1_{3A}$ distribution (Fig 6C). Indeed, GFP-$nsP1_{3A}$ remained detected as a diffuse cytoplasmic protein as observed in mock-treated cells thereby contrasting with the phenotype observed for GFP-nsP1. No colocalization of CD81 and GFP-$nsP1_{3A}$ fluorescence was observed (Fig 6D). Optical sectioning (z-stack) and three-dimensional (3D) volume reconstruction from image stacks confirmed that conversely to GFP-nsP1, GFP-$nsP1_{3A}$ poorly colocalized with CD81 in drug treated cells (Fig 6E and 6F). These phenotypes were confirmed from cells cultured with imipramine. According to these results, nsP1 behaves similarly to CD81 with regard to cholesterol storage, a property that requires the presence of palmitoylated cysteines in nsP1 C-terminus.

CHIKV nsP1 partitions with DRMs.

306 Given that nsP1 subcellular localization is sensitive to cholesterol redistribution to the PM, we
307 questioned its capacity to segregate with cholesterol-enriched membrane microdomains. Cholesterol
308 is not uniformly distributed in membranes. In living cells, it concentrates in nanoscale assemblies,
309 also enriched in sphingolipids and glycosylphosphatidylinositol (GPI)-anchored proteins, referred to
310 as lipid rafts. These compartments are characterized biochemically by their insolubility in non-ionic
311 detergents, a property reflected in their name (DRMs - detergent-resistant membrane
312 microdomains), and by their light density on sucrose gradients. Therefore, they can be separated
313 from non-raft membranes by centrifugation methods. Samples prepared from cells transfected with
314 GFP-nsP1 expression plasmid were treated with Triton X-100 at 4°C, separated on a 10-80% sucrose
315 density gradient, and then analyzed by western blot. Detergent-resistant fractions corresponding to
316 DRMs were identified utilizing an antibody against FLOT1, a well-known raft-associated protein (50).
317 In our experimental conditions, FLOT1 fractionated into light density fractions 1 and 2 at the top of
318 the gradient thereby identifying DRMs (Fig 7A). In contrast, the non-raft marker Na^+/K^+ ATPase
319 remained associated with fractions 7-9 of heavier density corresponding to non-raft membranes and
320 cytosolic compartment (detergent sensitive; DS). Using this protocol, more than 85% of the GFP-nsP1
321 protein was detected in FLOT1-positive fractions at the top of the gradient supporting its capacity to
322 associate with cholesterol-enriched DRMs (Fig 7A and 7B). To confirm GFP-nsP1 affinity for
323 cholesterol-enriched microdomains, this experiment was repeated starting from cells cultured in the
324 presence of the cholesterol depleting agent methyl-β-cyclodextrin (βMCD). Due to its ability to
325 sequester cholesterol in its hydrophobic pocket, βMCD extracts cholesterol from the lipid bilayer and
326 disrupts DRMs (51). Under these cholesterol depletion conditions, FLOT1 was redistributed from
327 DRMs to DS fractions and sedimented at the bottom of the density gradient (Fig 7C and 7D). Analysis
328 of the same fractions with anti-nsP1 antibodies revealed that GFP-nsP1 was barely detectable in top
329 fractions while it accumulated in fractions of heavier density together with FLOT1. Therefore, GFP-
330 nsP1 fractionation with DRMs is sensitive to cholesterol extraction from cell membranes. Finally, this
331 experiment was repeated starting from cells expressing GFP-nsP1$_{W258A}$ or GFP-nsP1$_{3A}$ mutant proteins

that displayed different sensitivity to U18666A. As observed for GFP-nsP1, the GFP-nsP1$_{W258A}$ mainly segregated with DRMs fractions attesting that raft association was not disrupted by mutation of W258 residue in the putative α-helix of nsP1 (Fig 7E and 7F). Analyzing the behavior of the GFP-nsP1$_{3A}$ mutant protein revealed, in contrast, that most of this protein was absent from the top fraction and co-segregated with the DS fractions. These experiments demonstrate that the presence of GFP-nsP1 in DRMs is mainly dictated by acylated cysteines while mutation in the putative α-helical peptide has only marginal impact on this phenotype.

nsPs associate with DRM fractions in cells with CHIKV RNA replication

Unlike SFV, CHIKV replication is completely abolished by nsP1$_{3A}$ mutation regardless of the type and growth temperature of cells (33, 34). In contrast, nsP1$_{W258A}$ mutation allows virus to grow efficiently in insect cells or in mammalian cells cultivated at 28^{o}C (33, 52). Combined with our observations, this strongly indicates that the presence of nsP1 in DRMs is an absolute requirement for CHIKV genome replication. Therefore, we questioned whether nsP1 affinity for DRMs was conserved in cells containing functional CHIKV replicase complexes. To this end, HEK293T cells either transfected with a trans-replication system that reproduces CHIKV RNA replication (Fig 2B) or infected with the CHIKV-LR-5'GFP were used. DRMs isolation followed by immunoblot analysis revealed that a significant fraction of nsP1 expressed in transfected or infected cells (~85 and ~40%, respectively) was detected in cholesterol-rich fractions (Fig 8D and 8E). NsP1 is the only alphavirus nonstructural protein with membrane affinity. In the replication complex, nsP1 co-localizes with nsP2, nsP3, and nsP4 (53–56). Thus, it is suspected to play a critical role in replication complex anchoring to the PM. Therefore, we investigated whether nsP1 capacity to segregate with DRMs has an impact on the association of other nsPs with specialized membrane microdomains. Probing gradient fractions prepared from transfected and infected cells with antibodies against nsPs established that a significant part of each of them was detected in DS fractions thereby agreeing with the previously reported capacity of nsPs to be present in different cytosolic compartments (57). However, approximately 10-30 % of total

nsP3 and nsP4 levels were also present in raft fractions. In some, but not in all experiments, nsP2 was also detectable in DRMs; most probably reflecting the weaker interaction of nsP2 with other components of replicase complexes. In order to further assess the relevance for the presence of nsP2, nsP3 and nsP4 in DRMs fractions, these experiments were reproduced starting from cells transfected with a CHIKV trans-replicase system in which the nsP1 protein contained the $C_{418\text{-}420}A$ mutation. As expected, this mutation prevented nsP1 association with DRMs (Fig 8C). Concomitantly, nsP2, nsP3 and nsP4 were also excluded from these fractions. Altogether these results confirm the capacity of nsP1, expressed in the context of trans-replicase or by infectious CHIKV, to associate with DRMs, an association that dictates targeting of other nsPs, albeit at low levels, to cholesterol-enriched membrane microdomain. Furthermore, the $C_{418\text{-}420}A$ mutation that completely inactivates CHIKV trans-replicase (33) completely prevented association of CHIKV nsPs with DRMs.

Conservation of nsP1-directed cholesterol affinity among divergent Old World alphaviruses.

Despite the presence of palmitoylated cysteine residues in the C-terminal region of nsP1 is a conserved feature of distantly related Old World alphaviruses (30, 34), functional studies have highlighted differences with regard to cysteine requirement for genome replication. Cysteine-to-alanine mutation are lethal for CHIKV (33, 34) but is well tolerated by SINV (30). In the light of such differences and of the herein evidenced role of the CHIKV nsP1 cysteines in lipid raft association, we next questioned whether SINV nsP1 behaves similarly with respect to cholesterol. To achieve this, a plasmid encoding a GFP-fused SINV nsP1 protein was generated (Fig 9A) and used for the transfection of HEK293T cells. Then, we tested SINV nsP1 partitioning to DRMs by membrane flotation assays. As previously observed for CHIKV nsP1, SINV nsP1 was also detected in the top fractions of the density gradient supporting its ability to partition with cholesterol-rich membrane microdomains. However, contrasting with CHIKV for which almost 85% of nsP1 associated to DRM fractions, a roughly equal proportion of the SINV nsP1 was associated with DRMs and DS (Fig 9B). We further investigated SINV GFP-nsP1 affinity for cholesterol by testing its sensitivity to U18666A in

382 confocal microscopy experiments. In control conditions, SINV GFP-nsP1 was detected at the PM,
383 including in filopodia-like membrane protrusions that were abundantly observed as reported before
384 for the untagged protein (42) and for CHIKV GFP-nsP1 (Fig 9C). In the presence of U18666A, SINV
385 GFP-nsP1 was still mainly detected at the PM, while cholesterol stained with filipin was concentrated
386 in intracellular storage compartments as expected. In these conditions, co-localization of GFP-nsP1
387 SINV with cholesterol-enriched endosomes was unfrequently detected. This is in contrast with the
388 results obtained for CHIKV nsP1 (Fig 4D) (Mander's coefficient of 0.394 ± 0.032 and 0.217 ± 0.001 for
389 CHIKV and SINV nsP1 respectively). Next, we investigated the role of palmitoylated cysteine by
390 repeating these experiments starting from cells expressing a cysteine-to-alanine SINV nsP1
391 palmitoylation-negative mutant protein (GFP-nsP1$_{C420A}$). As shown in Figure 9B, the DRMs association
392 of GFP-nsP1$_{C420A}$ was significantly reduced when compared with that of SINV GFP-nsP1 (Fig 8A).
393 Analyzing SINV GFP-nsP1 $_{C420A}$ subcellular localization in U18666A treated cells confirmed that this
394 mutant did not colocalize with filipin-labelled cholesterol (Fig 9D). Altogether these results suggest
395 that SINV nsP1 is targeted to DRMs, a property that depends of palmitoylated cysteine as previously
396 observed for CHIKV nsP1. However, compared with CHIKV counterpart, SINV nsP1 is equally
397 abundant in DS compartments and displays only modest sensitivity to U18666A suggesting a reduced
398 affinity for cholesterol.

399 **Discussion**

400 The present study identifies CHIKV nsP1 as a lipid-raft co-segregating protein with an affinity for
401 cholesterol. We defined cysteine residues that can be palmitoylated as the molecular determinant
402 important for this targeting. In the context of cells with ongoing CHIKV RNA replication, nsP1,
403 together with a fraction of other nsPs, partitions with cholesterol-rich DRMs. Together with evidence
404 that drugs reducing cholesterol availability at the PM impair CHIKV RNA replication, our results
405 support that nsP1 targeting to cholesterol-rich PM microdomains may have a functional importance
406 for viral genome replication.

Cholesterol is a main component of membranes. Together with sphingolipids, it segregates into discrete microdomains, referred to as lipid rafts or DRMs, present both on the inner and the outer leaflet of the PM (58, 59). These membrane domains with a size on the nm scale are highly dynamic. They accumulate a subset of membrane proteins, mainly GPI-anchored proteins, transmembrane proteins, and acylated cell components (60, 61). Based on these properties, rafts were seen as platforms that compartmentalize cellular processes with an important function in receptor-ligand interaction, signal transduction and endocytosis (60). Herein, we establish that CHIKV nsP1 associates with the PM. In this compartment, a pool of nsP1 is targeted to cholesterol-containing DRMs (Fig 10a), an association that was reversed by βMCD cholesterol-removal agent. Affinity for cholesterol was further supported by investigating nsP1 behavior with regard to U18666A- or imipramine-mediated cholesterol sequestration in LE/Ls. We found that intracellular cholesterol storage resulted in nsP1 accumulation in endosomes without consequence on overall nsP1 membrane binding ability (Fig 10b). Altogether these results indicate that availability of cholesterol at the PM is required for appropriate targeting of CHIKV nsP1 to this compartment.

In the last decade, the biochemical or biophysical underpinnings that govern nsP1 association with membranes have been the focus of an intense attention. For SFV and SINV, the central α-helical motif in nsP1 spanning amino acid residues 245 to 264 was proposed as the main determinant for membrane anchoring to lipid bilayers with W259 residue being critical for hydrophobic interactions with the phospholipid acyl chains (25). Conserved acylated cysteine(s) in nsP1 were proposed to tighten this membrane interaction (26, 27, 30, 34). Using cell fractionation assays, we show that both $W_{258}A$ substitution in the putative α-helix of CHIKV nsP1 and $C_{417\text{-}419}A$ mutations indeed decrease nsP1 affinity for cell membranes. Interestingly, combining $W_{258}A$ and $C_{417\text{-}419}A$ mutations further reduced nsP1 membrane association thereby suggesting that in the CHIKV nsP1 the two domains may synergize for membrane interaction, a situation that was not described for other alphaviruses. Analyzing the contribution of these membrane interaction determinants in nsP1 targeting to lipid

rafts revealed that the $W_{258}A$ mutation had only a slight effect on nsP1 co-fractionation with cholesterol-rich domains. This mutation also slightly reduced PM association of nsP1 and facilitated its association with internal membranes. This may indicate that W258 residue is important for membrane/plasma membrane targeting of nsP1 but not for its palmitoylation, DRMs association and enzymatic activity. How these properties correlate with the proposed role of W258 residue as one of membrane anchors of nsP1 is currently unclear. For the proper understanding of the somewhat controversial data regarding the importance of the W258 residue, the structure of the membrane bound α-helical peptide of nsP1 (25) should be compared with the structure of membrane-bound enzymatically active nsP1 which, to this date, is not available. In contrast to the $W_{258}A$ mutation the effects of the $C_{417\text{-}419}A$ mutation on CHIKV nsP1 were unambiguous. This mutation, previously reported to prevent CHIKV nsP1 palmitoylation and replication (33, 34), dramatically reduced DRMs co-fractionation (Fig 10c). Moreover, by contrast with wild-type nsP1, $nsP1_{C417\text{-}419A}$ sequestration with Lamp2 in endosomes could not be observed under U18666A or imipramine treatment. According to these experiments, acylation appears as critical to direct nsP1 to cholesterol-enriched membrane microdomains. This result parallels previous evidence regarding the role of palmitoylation in cellular ($p59^{fyn}$ and $p60^{src}$) (62) or viral (influenza hemagglutinin) (63) proteins association with rafts. This observation raised the question of the functional outcome of nsP1 association with cholesterol-rich DRMs.

Because other nonstructural proteins of alphaviruses cannot directly associate with membranes, nsP1 plays a decisive role in proper targeting and membrane binding of other nsPs involved in the formation and functioning of alphavirus replication complex (24). Starting from cells infected with CHIKV, we found that a fraction of each of the four nsPs was associated with DRMs. These results were confirmed in cells transfected with plasmids encoding fora CHIKV trans-replication system, in which other non-structural proteins co-sedimented with DRMs depending on the integrity of nsP1 C417-419 residues. Currently the functional importance of nsPs targeting to rafts is unknown. Nevertheless, we observed that in addition to nsP1 sequestration into late endosomes, U18666A and

458 imipramine also generated a significant drop in CHIKV genome replication. This raises the question of
459 the functional consequences of nsP1 mistargeting and of its impact on replication complex assembly.

460 Over two decades, alphaviruses encoding nsP1 mutants with reduced membrane binding ability have
461 been in the focus of different studies. They established that nsP1 palmitoylation had only a mild
462 impact on SINV or SFV infectivity, highlighting the essential role of the W259 residue in nsP1's central
463 α-helix for both membrane anchoring and genome replication (30, 31). For CHIKV, the $W_{258}A$ mutant
464 is viable, albeit having a temperature-sensitive phenotype (33). By contrast, the $C_{417\text{-}419}A$ mutation
465 results in complete inactivation of the CHIKV replicase, leading to non-functional enzymes unable to
466 synthesize any viral RNAs both in mammalian and insect cells (33, 34, 52). Here, the direct
467 comparison of SINV and CHIKV revealed that SINV nsP1 partitions with DRMs but to a lesser extent
468 than observed for CHIKV nsP1. This phenotype was equally dependent upon conserved cysteine in
469 nsP1. Moreover, SINV nsP1 targeting to the PM was less sensitive to cholesterol manipulation by
470 U18666A. These discrepancies therefore parallel the differences in nsP1 palmitoylation requirement
471 previously reported for CHIKV and SINV replication (33). However, counterintuitively, SINV genome
472 replication was also sensitive to U18666A and cholesterol sequestration (this study and (35)) albeit
473 less than observed for CHIKV (data not shown). Conversely to CHIKV, this might not reflect
474 dependency on PM rafts, but instead cholesterol-induced alteration of endosomes where SINV
475 preferentially replicates as proposed by others (35, 64).

476 In the last decade, cholesterol-rich membrane microdomains, beyond their role in virus entry and
477 exit, have also been identified as platforms for the assembly and anchoring of replication complexes
478 produced by a broad range of RNA viruses including HCV, picornaviruses or flaviviruses (9, 10, 12, 18,
479 65). A dramatic reduction of viral RNA replication was observed upon membrane cholesterol
480 extraction or in conditions reducing cholesterol availability (12, 14, 66, 67) establishing functional
481 importance for this association. Besides changing membrane composition and fluidity, which may
482 affect different interactions between virus-encoded replicase subunits, cholesterol partitioning in

membranes also attract cellular proteins, with functions in cell signaling and intracellular trafficking. We can assume that targeting CHIKV nsP1 and possibly other nsPs at these sites may favor interaction with raft-associated cellular factors indispensable for viral replication. The exact necessity for nsP1 partitioning to DRMs therefore will deserve further investigations.

Materials and Methods

Antibodies and reagents: The following antibodies/reagents and respective dilutions were used in this study: rabbit polyclonal antisera against CHIKV nsP1, nsP2, nsP3, nsP4 (all in-house, 1:1,000), monoclonal antibodies against GAPDH (1:1,000) (Santa Cruz Biotechnologies Inc.), Na^+ K^+ ATPase (1:50,000) (Ab76020, Abcam), GFP (1:1,000) (Chromotek), Lamp2 (1:1,000), CD81 (1:500) (Clone JS-81, BD Biosciences) and flotillin-1 (1:1,000) (BD Biosciences). Secondary antibodies conjugated to horseradish peroxidase or Alexa Fluor were purchased from Jackson Immunoresearch and Thermo Fisher Scientific, respectively. Filipin III, U18666A, Lovastatin, methyl-β-cyclodextrin were purchased from Sigma-Aldrich. Imipramine was obtained from Abcam and WGA-647 from Thermo Fisher Scientific.

Cells: HEK293T cells (ATCC # ACS-4500), HeLa cells (ATCC # CRM-CCL2), BHK21 cells (ATCC # CCL-10) and U2OS cells (ATCC # HTB-96) used for propagation and Vero cells (ATCC # CCL-81) used for titration of the CHIKV were cultured in Dulbecco's modified Eagle's medium (DMEM, Thermo Fischer Scientific) supplemented with penicillin and 10% fetal calf serum (FCS, Lonza) and grown at 37°C in a 5% CO_2 atmosphere. Viability of cells incubated with drugs for 24 hrs was measured using Cell Titer 96 Aqueous one solution cell proliferation assay (Promega) according to the manufacturer's protocol.

Viruses: The pCHIKV-LR-5'GFP, full-length molecular clone of CHIKV (LR2006OPY1 strain) with GFP reporter (68), was linearized and transcribed *in vitro* using the mMESSAGE mMACHINE kit (Ambion-

Life Technologies). 1 µg of RNA was then transfected with lipofectamine 2000 (Thermo Fisher Scientific) into 10^5 HEK293T cells and the cells were incubated at 37°C for 24 hrs. Culture medium was collected, and virus stock was amplified on BHK-21 cells. After 48 hrs at 37°C, the supernatant was collected, filtered through a 0.45 µm membrane, aliquoted and stored at -80°C. Viral stocks were tittered using plaque assay as previously reported (39).

Infection with CHIKV-reporter viruses: The cells (70-80% confluence) were rinsed once with PBS before infection with CHIKV-LR-5'GFP diluted to achieve the desired MOI. For pre-infection experiments, the cells were pre-incubated with the virus for 1 hr or 2 hrs before drug addition. For post-infection experiments, the cells were incubated with drugs for 30 min before infection. After 24 hrs in culture, the cells were lysed with RIPA buffer. GFP reporter fluorescence was measured directly from the cell lysate using an Infinite F200PRO fluorometer (Tecan). Values were normalized to the protein content in the sample determined using the BCA Assay (Pierce).

Plasmids and transfection: Sequence encoding for CHIKV nsP1 was amplified by PCR using pCHIKV-LR-5'GFP as a template; obtained fragment was cloned into the pEGFP-C1 plasmid as previously described (69). Sequences encoding for a $nsP1_{W258A}$, $nsP1_{C417-419A}$ and $nsP1_{DM}$ were generated using the Quikchange site-directed mutagenesis kit by Agilent. SINV nsP1 and $nsP1_{420A}$ were obtained using PCR and pTOTO1101 (70) or its derivative pSINV-C_{420}A1 (30) as templates. These inserts were cloned in frame with eGFP in the peGFP-C1 plasmid. Cells were transfected with obtained plasmids using JetPei reagent (Polyplus Transfection) according to manufacturer recommendations.

Trans-replication assay: For trans-replication assays, CMV-P1234 (71) or CMV-SINV-P1234 (72) plasmids encoding nonstructural polyprotein from CHIKV or SINV respectively were cotransfected together with the HSPolI-Fluc-Gluc (33) or HSPolI-SINV-tFluc-Gluc (73) template plasmids encoding for replication-competent template RNA of CHIKV or SINV containing firefly and *Gaussia* luciferase reporter sequences placed under control of genomic and subgenomic promoters respectively. Equal amounts of plasmids were transfected into HEK293T cells using JetPei transfection reagent. After 24

hrs in culture, cells were washed in PBS and lysed using Passive Lysis Buffer (Promega). Expression of firefly and *Gaussia* luciferase was determined using the Dual-Glo Luciferase Assay system (Promega) and a Spark luminometer (Tecan). Reporter activities were normalized to the protein content in the sample determined using the BCA Assay (Pierce).

Immunoblotting: Samples were separated by SDS-PAGE and then transferred to PVDF membrane (Hybond, Amersham). Membranes were blocked using 5% non-fat dry milk in PBS and probed with appropriate primary antibodies. After wash steps with PBS – 0.1% Tween 20, the membranes were probed with HRP-conjugated secondary antibodies. The revelation was performed by incubating the membranes with either Luminata Forte (Merck) or Clarity Max (BioRad) and then image acquisition was done using a Chemidoc (Bio-Rad).

Cell fractionation and membrane flotation assays: Cells were incubated in hypotonic buffer (10mM Tris/HCl [pH 7.4], 10 mM NaCl supplemented with protease inhibitors) for 10 min on ice and then lysed with a Dounce homogenizer (30-40 strokes). The lysates were clarified by low-speed centrifugation at 1,000 g for 10 min. Obtained post-nuclear supernatants (PNS) were then adjusted to a final concentration of 500 mM NaCl and incubated for 30 min on ice. After ultracentrifugation at 25,000 g for 20 min, the cytosolic (supernatant, S25) and membrane fraction (pellet, P25) were collected. P25 samples were solubilized in lysis buffer composed of 1% Brij 96 in 20 mM Tris/HCl [pH 7.5] before analysis. For membrane flotation experiments, cells were resuspended in 250 mM sucrose in PBS supplemented with protease inhibitors and then lysed with a Dounce homogenizer (30-40 strokes). Cell lysates were spun at 1,000 g for 10 min to pellet the nuclei. The supernatant referred to as crude lysate (CL) was then adjusted to 30% iodixanol concentration by mixing Optiprep (Axis-Shield). CL (4 mL) was loaded at the bottom of a centrifuge tube, and then overlaid with 4 mL 20% iodixanol and then 4 mL 10% iodixanol. The gradient was then spun 200,000 g at 4°C for 16 hrs in a Beckman SW41 rotor. Finally, 24 fractions were collected from top to bottom.

Detergent-resistant membrane isolation: Cells were lysed on ice in TNE buffer (10 mM Tris/HCl [pH 7.5], 100 mM NaCl, 10 mM EDTA) containing 0.5% Triton X-100 for 30 min. Lysates were then further treated with the Dounce homogenizer, and then clarified by low-speed centrifugation at 1,000 g for 10 min to obtain the PNS. PNS (0.5 mL) was adjusted to 60% sucrose by adding 1.5 mL of 80% sucrose TNE (w/v). The lysates were layered over 500 µL of 80% sucrose TNE, then covered with 2 mL of 50% sucrose TNE, 6 mL of 38% sucrose TNE, and 1.5 mL of 10% sucrose TNE. The sucrose gradients were centrifuged at 100,000 g at 4°C for 18 hrs in a Beckman SW41 rotor (Beckman Coulter). Nine fractions were then collected and analyzed by immunoblotting.

Immunofluorescence microscopy and image analysis: Cells grown on glass coverslips were washed with PBS and then fixed with 4% paraformaldehyde/PBS (Sigma Aldrich) for 10 min. For intracellular labeling, the cells were permeabilized with 0.1% Triton-X100 in PBS and blocked for 30 min with PBS containing 0.2% Bovine Serum Albumin. Incubation with primary antibody was performed for 1 hr. After washes with PBS, secondary reagents were added for 30 min. DAPI (Sigma-Aldrich) was used to stain the nuclei. Filipin or WGA-647 staining was performed by incubation at room temperature for either 1 hr or 10 min respectively. After final washes, coverslips were mounted with Prolong Gold antifade mounting media (Thermo Fisher Scientific). Images were acquired using a Leica SP5-SMD scanning confocal microscope equipped with a 63×, 1.4 numerical aperture Leica Apochromat oil lense at the Montpellier Resources Imaging platform. Image analysis was performed utilizing Fiji ImageJ and the JACoP plugin. For Mander's analysis, the threshold and region of interest were maintained consistent between the different conditions. 3D reconstruction was performed by Imaris software.

Statistical analysis: All of the analyses (unpaired Student's t-test) were performed using GraphPad Prism version 6 (GraphPad Software Inc.). A p-value of <0.05 was considered statistically significant. Following designations are used on figures: * $p<0.05$; ** $p<0.001$; ***$p<0.0001$; **** $p<0.0001$.

Acknowledgments

We are indebted to Fabien Blanchet for helpful discussions and Joe McKellar for manuscript edition (IRIM, Montpellier, France), to Cécile Gauthier-Rouvière (CRBM, Montpellier, France) for reagents and to the Montpellier RIO Imaging platform staff for technical assistance.

Authors contribution

Conceptualization: LB, AM; *Methodology*: LB; *Funding acquisition*: LB; *Investigation-main experiments*: WB. *Investigations - additional experiments*: AN, EB; *Supervision*: LB; *Writing original draft*: LB, AM, WB.

Financial disclosure statement

The funders had no role in study design, data collection and interpretation, or the decision to submit the work for publication.

Funding

This work was funded by the Agence Nationale de la Recherche (ANR-18-CE11-0026-01). WB is a fellow of Montpellier Méditerranée Infections – Infectiopôle Sud foundation

Competing interests

The authors have declared that no competing interests exist.

References

1. Lorizate M, Kräusslich H-G. 2011. Role of Lipids in Virus Replication. Cold Spring Harb Perspect Biol 3:a004820.
2. Paul D, Bartenschlager R. 2013. Architecture and biogenesis of plus-strand RNA virus replication factories. World J Virol 2:32–48.
3. Sasvari Z, Nagy PD. 2010. Making of viral replication organelles by remodeling interior membranes. Viruses 2:2436–42.
4. de Castro IF, Volonte L, Risco C. 2013. Virus factories: biogenesis and structural design. Cell Microbiol 15:24–34.

5. Goldstein JL, Brown MS. 1984. Progress in understanding the LDL receptor and HMG-CoA reductase, two membrane proteins that regulate the plasma cholesterol. J Lipid Res 25:1450–1461.

6. Infante RE, Wang ML, Radhakrishnan A, Kwon HJ, Brown MS, Goldstein JL. 2008. NPC2 facilitates bidirectional transfer of cholesterol between NPC1 and lipid bilayers, a step in cholesterol egress from lysosomes. Proc Natl Acad Sci USA 105:15287–15292.

7. Mercer J, Schelhaas M, Helenius A. 2010. Virus entry by endocytosis. Annu Rev Biochem 79:803–33.

8. Stoeck IK, Lee JY, Tabata K, Romero-Brey I, Paul D, Schult P, Lohmann V, Kaderali L, Bartenschlager R. 2018. Hepatitis C Virus Replication Depends on Endosomal Cholesterol Homeostasis. J Virol 92.

9. Aizaki H, Lee K-J, Sung VM-H, Ishiko H, Lai MMC. 2004. Characterization of the hepatitis C virus RNA replication complex associated with lipid rafts. Virology 324:450–461.

10. Shi ST, Lee K-J, Aizaki H, Hwang SB, Lai MMC. 2003. Hepatitis C Virus RNA Replication Occurs on a Detergent-Resistant Membrane That Cofractionates with Caveolin-2. J Virol 77:4160–4168.

11. Mackenzie JM, Khromykh AA, Parton RG. 2007. Cholesterol manipulation by West Nile virus perturbs the cellular immune response. Cell Host Microbe 2:229–39.

12. Ilnytska O, Santiana M, Hsu NY, Du WL, Chen YH, Viktorova EG, Belov G, Brinker A, Storch J, Moore C, Dixon JL, Altan-Bonnet N. 2013. Enteroviruses harness the cellular endocytic machinery to remodel the host cell cholesterol landscape for effective viral replication. Cell Host Microbe 14:281–93.

13. Xu K, Nagy PD. 2015. RNA virus replication depends on enrichment of phosphatidylethanolamine at replication sites in subcellular membranes. P Natl Acad Sci USA 112:E1782–E1791.

14. Albulescu L, Wubbolts R, van Kuppeveld FJ, Strating JR. 2015. Cholesterol shuttling is important for RNA replication of coxsackievirus B3 and encephalomyocarditis virus. Cell Microbiol 17:1144–56.

15. Rothwell C, LeBreton A, Young Ng C, Lim JYH, Liu W, Vasudevan S, Labow M, Gu F, Gaither LA. 2009. Cholesterol biosynthesis modulation regulates dengue viral replication. Virology 389:8–19.

16. Wichit S, Hamel R, Bernard E, Talignani L, Diop F, Ferraris P, Liegeois F, Ekchariyawat P, Luplertlop N, Surasombatpattana P, Thomas F, Merits A, Choumet V, Roques P, Yssel H, Briant L, Misse D. 2017. Imipramine Inhibits Chikungunya Virus Replication in Human Skin Fibroblasts through Interference with Intracellular Cholesterol Trafficking. Sci Rep 7:3145.

17. Takano T, Endoh M, Fukatsu H, Sakurada H, Doki T, Hohdatsu T. 2017. The cholesterol transport inhibitor U18666A inhibits type I feline coronavirus infection. Antiviral Research 145:96–102.

18. Sagan SM, Rouleau Y, Leggiadro C, Supekova L, Schultz PG, Su AI, Pezacki JP. 2006. The influence of cholesterol and lipid metabolism on host cell structure and hepatitis C virus replication. Biochem Cell Biol 84:67–79.

19. Weaver SC, Lecuit M. 2015. Chikungunya Virus and the Global Spread of a Mosquito-Borne Disease. N Engl J Med 372:1231–1239.

20. Froshauer S, Kartenbeck J, Helenius A. 1988. Alphavirus RNA replicase is located on the cytoplasmic surface of endosomes and lysosomes. J Cell Biol 107:2075–86.

21. Kujala P, Ikaheimonen A, Ehsani N, Vihinen H, Auvinen P, Kaariainen L. 2001. Biogenesis of the Semliki Forest virus RNA replication complex. J Virol 75:3873–84.

22. Spuul P, Balistreri G, Hellstrom K, Golubtsov AV, Jokitalo E, Ahola T. 2011. Assembly of alphavirus replication complexes from RNA and protein components in a novel trans-replication

system in mammalian cells. J Virol 85:4739–51.

23. Ahola T, Kaariainen L. 1995. Reaction in alphavirus mRNA capping: formation of a covalent complex of nonstructural protein nsP1 with 7-methyl-GMP. P Natl Acad Sci USA 92:507–11.
24. Salonen A, Vasiljeva L, Merits A, Magden J, Jokitalo E, Kaariainen L. 2003. Properly folded nonstructural polyprotein directs the semliki forest virus replication complex to the endosomal compartment. J Virol 77:1691–702.
25. Lampio A, Kilpelainen I, Pesonen S, Karhi K, Auvinen P, Somerharju P, Kaariainen L. 2000. Membrane binding mechanism of an RNA virus-capping enzyme. J Biol Chem 275:37853–9.
26. Spuul P, Salonen A, Merits A, Jokitalo E, Kaariainen L, Ahola T. 2007. Role of the amphipathic peptide of Semliki forest virus replicase protein nsP1 in membrane association and virus replication. J Virol 81:872–83.
27. Laakkonen P, Ahola T, Kaariainen L. 1996. The effects of palmitoylation on membrane association of Semliki forest virus RNA capping enzyme. J Biol Chem 271:28567–71.
28. Ahola T, Lampio A, Auvinen P, Kaariainen L. 1999. Semliki Forest virus mRNA capping enzyme requires association with anionic membrane phospholipids for activity. EMBO J 18:3164–72.
29. Tomar S, Narwal M, Harms E, Smith JL, Kuhn RJ. 2011. Heterologous production, purification and characterization of enzymatically active Sindbis virus nonstructural protein nsP1. Protein Expr Purif 79:277–84.
30. Ahola T, Kujala P, Tuittila M, Blom T, Laakkonen P, Hinkkanen A, Auvinen P. 2000. Effects of Palmitoylation of Replicase Protein nsP1 on Alphavirus Infection. Journal of Virology 74:6725–6733.
31. Zusinaite E, Tints K, Kiiver K, Spuul P, Karo-Astover L, Merits A, Sarand I. 2007. Mutations at the palmitoylation site of non-structural protein nsP1 of Semliki Forest virus attenuate virus replication and cause accumulation of compensatory mutations. J Gen Virol 88:1977–85.
32. Karo-Astover L, Šarova O, Merits A, Žusinaite E. 2010. The infection of mammalian and insect cells with SFV bearing nsP1 palmitoylation mutations. Virus Research 153:277–287.
33. Age Utt, Rausalu K, Jakobson M, Männik A, Alphey L, Fragkoudis R, Merits A. 2019. Design and use of Chikungunya virus replication templates utilizing mammalian and mosquito RNA polymerase I mediated transcription. Journal of Virology JVI.00794-19.
34. Zhang N, Zhao H, Zhang L. 2019. Fatty Acid Synthase Promotes the Palmitoylation of Chikungunya Virus nsP1. Journal of Virology 93:e01747-18.
35. Ng CG, Coppens I, Govindarajan D, Pisciotta J, Shulaev V, Griffin DE. 2008. Effect of host cell lipid metabolism on alphavirus replication, virion morphogenesis, and infectivity. P Natl Acad Sci USA 105:16326–31.
36. Alberts AW. 1990. Lovastatin and Simvastatin - Inhibitors of HMG CoA Reductase and Cholesterol Biosynthesis. CRD 77:14–21.
37. Sobo K, Blanc IL, Luyet P-P, Fivaz M, Ferguson C, Parton RG, Gruenberg J, Goot FG van der. 2007. Late Endosomal Cholesterol Accumulation Leads to Impaired Intra-Endosomal Trafficking. PLOS ONE 2:e851.
38. Cenedella RJ. 2009. Cholesterol Synthesis Inhibitor U18666A and the Role of Sterol Metabolism and Trafficking in Numerous Pathophysiological Processes. Lipids 44:477–487.
39. Bernard E, Solignat M, Gay B, Chazal N, Higgs S, Devaux C, Briant L. 2010. Endocytosis of Chikungunya Virus into Mammalian Cells: Role of Clathrin and Early Endosomal Compartments. PLoS ONE 5.
40. Lu YE, Cassese T, Kielian M. 1999. The cholesterol requirement for sindbis virus entry and exit

and characterization of a spike protein region involved in cholesterol dependence. J Virol 73:4272–8.

41. Barton DJ, Sawicki SG, Sawicki DL. 1991. Solubilization and immunoprecipitation of alphavirus replication complexes. J Virol 65:1496–506.

42. Laakkonen P, Auvinen P, Kujala P, Kaariainen L. 1998. Alphavirus replicase protein NSP1 induces filopodia and rearrangement of actin filaments. J Virol 72:10265–9.

43. Peranen J, Laakkonen P, Hyvonen M, Kaariainen L. 1995. The alphavirus replicase protein nsP1 is membrane-associated and has affinity to endocytic organelles. Virology 208:610–20.

44. Dermine J-F, Duclos S, Garin J, St-Louis F, Rea S, Parton RG, Desjardins M. 2001. Flotillin-1-enriched Lipid Raft Domains Accumulate on Maturing Phagosomes. J Biol Chem 276:18507–18512.

45. Lu F, Liang Q, Abi-Mosleh L, Das A, De Brabander JK, Goldstein JL, Brown MS. 2015. Identification of NPC1 as the target of U18666A, an inhibitor of lysosomal cholesterol export and Ebola infection. eLife 4:e12177.

46. Schroeder F, Holland JF, Bieber LL. 1971. Fluorometric evidence for the binding of cholesterol to the filipin complex. J Antibiot 24:846–849.

47. Liscum L, Faust JR. 1989. The intracellular transport of low density lipoprotein-derived cholesterol is inhibited in Chinese hamster ovary cells cultured with 3-beta-[2-(diethylamino)ethoxy]androst-5-en-17-one. J Biol Chem 264:11796–11806.

48. Charollais J, Goot FGVD. 2009. Palmitoylation of membrane proteins (Review). Molecular Membrane Biology 26:55–66.

49. Charrin S, Manié S, Thiele C, Billard M, Gerlier D, Boucheix C, Rubinstein E. 2003. A physical and functional link between cholesterol and tetraspanins. European Journal of Immunology 33:2479–2489.

50. Eckert GP, Igbavboa U, Müller WE, Wood WG. 2003. Lipid rafts of purified mouse brain synaptosomes prepared with or without detergent reveal different lipid and protein domains. Brain Research 962:144–150.

51. Christian AE, Haynes MP, Phillips MC, Rothblat GH. 1997. Use of cyclodextrins for manipulating cellular cholesterol content. J Lipid Res 38:2264–2272.

52. Bartholomeeusen K, Utt A, Coppens S, Rausalu K, Vereecken K, Arien KK, Merits A. 2018. A Chikungunya Virus trans-Replicase System Reveals the Importance of Delayed Nonstructural Polyprotein Processing for Efficient Replication Complex Formation in Mosquito Cells. J Virol 92.

53. Rana J, Rajasekharan S, Gulati S, Dudha N, Gupta A, Chaudhary VK, Gupta S. 2014. Network mapping among the functional domains of Chikungunya virus nonstructural proteins. Proteins 82:2403–11.

54. Sreejith R, Rana J, Dudha N, Kumar K, Gabrani R, Sharma SK, Gupta A, Vrati S, Chaudhary VK, Gupta S. 2012. Mapping interactions of Chikungunya virus nonstructural proteins. Virus Res 169:231–6.

55. Kumar S, Kumar A, Mamidi P, Tiwari A, Kumar S, Mayavannan A, Mudulli S, Singh AK, Subudhi BB, Chattopadhyay S. 2018. Chikungunya virus nsP1 interacts directly with nsP2 and modulates its ATPase activity. Scientific Reports 8:1045.

56. Remenyi R, Gao Y, Hughes RE, Curd A, Zothner C, Peckham M, Merits A, Harris M. 2018. Persistent Replication of a Chikungunya Virus Replicon in Human Cells Is Associated with Presence of Stable Cytoplasmic Granules Containing Nonstructural Protein 3. J Virol 92.

57. Pietila MK, Albulescu IC, Hemert MJV, Ahola T. 2017. Polyprotein Processing as a Determinant for in Vitro Activity of Semliki Forest Virus Replicase. Viruses 9.

58. Lingwood D, Simons K. 2010. Lipid Rafts As a Membrane-Organizing Principle. Science 327:46–50.

59. Hancock JF, Parton RG. 2005. Ras plasma membrane signalling platforms. Biochemical Journal 389:1–11.

60. Simons K, Ikonen E. 1997. Functional rafts in cell membranes. Nature 387:569–572.

61. Levental I, Lingwood D, Grzybek M, Coskun Ü, Simons K. 2010. Palmitoylation regulates raft affinity for the majority of integral raft proteins. PNAS 107:22050–22054.

62. Shenoy-Scaria AM, Dietzen DJ, Kwong J, Link DC, Lublin DM. 1994. Cysteine3 of Src family protein tyrosine kinase determines palmitoylation and localization in caveolae. The Journal of Cell Biology 126:353–363.

63. Sobocińska J, Roszczenko-Jasińska P, Ciesielska A, Kwiatkowska K. 2018. Protein Palmitoylation and Its Role in Bacterial and Viral Infections. Front Immunol 8.

64. Thaa B, Biasiotto R, Eng K, Neuvonen M, Gotte B, Rheinemann L, Mutso M, Utt A, Varghese F, Balistreri G, Merits A, Ahola T, McInerney GM. 2015. Differential Phosphatidylinositol-3-Kinase-Akt-mTOR Activation by Semliki Forest and Chikungunya Viruses Is Dependent on nsP3 and Connected to Replication Complex Internalization. J Virol 89:11420–37.

65. Cordero JG, Juárez ML, González-Y-Merchand JA, Barrón LC, Castañeda BG. 2014. Caveolin-1 in Lipid Rafts Interacts with Dengue Virus NS3 during Polyprotein Processing and Replication in HMEC-1 Cells. PLOS ONE 9:e90704.

66. Paul D, Hoppe S, Saher G, Krijnse-Locker J, Bartenschlager R. 2013. Morphological and biochemical characterization of the membranous hepatitis C virus replication compartment. J Virol 87:10612–27.

67. Ye J, Wang C, Sumpter R, Brown MS, Goldstein JL, Gale M. 2003. Disruption of hepatitis C virus RNA replication through inhibition of host protein geranylgeranylation. PNAS 100:15865–15870.

68. Vanlandingham DL, Tsetsarkin K, Hong C, Klingler K, McElroy KL, Lehane MJ, Higgs S. 2005. Development and characterization of a double subgenomic chikungunya virus infectious clone to express heterologous genes in Aedes aegypti mosquitoes. Insect Biochem Mol Biol 35:1162–70.

69. Matkovic R, Bernard E, Fontanel S, Eldin P, Chazal N, Hassan Hersi D, Merits A, Peloponese JM, Briant L. 2018. The host DHX9 DExH Box helicase is recruited to Chikungunya virus replication complexes for optimal genomic RNA translation. J Virol.

70. Polo JM, Davis NL, Rice CM, Huang HV, Johnston RE. 1988. Molecular analysis of Sindbis virus pathogenesis in neonatal mice by using virus recombinants constructed in vitro. Journal of Virology 62:2124–2133.

71. Utt A, Quirin T, Saul S, Hellstrom K, Ahola T, Merits A. 2016. Versatile Trans-Replication Systems for Chikungunya Virus Allow Functional Analysis and Tagging of Every Replicase Protein. PLoS ONE 11:e0151616.

72. Götte B, Utt A, Fragkoudis R, Merits A, McInerney GM. 2020. Sensitivity of alphaviruses to G3BP deletion correlates with efficiency of replicase polyprotein processing. Journal of Virology.

73. Götte B, Utt, Age, Fragkoudis , Rennos, Merits, Andres, McInerney, Gerald M. Submitted to Journal of Virology JVI01681-19R1. Sensitivity of alphaviruses to G3BP deletion correlates with efficiency of replicase polyprotein processing.

Figure legends

Figure 1: Cholesterol homeostasis regulates CHIKV life cycle

(A) Cholesterol metabolism and biosynthesis inhibitors. (B) Drugs affecting cholesterol metabolism inhibit CHIKV infection. HEK293T cells treated for 30 min with the indicated concentrations of (a) lovastatin, (c) U18666A, (e) imipramine were infected with CHIKV-LR-5'GFP at a MOI of 0.5. Infection was monitored after 24 hrs by quantification of GFP reporter in the cell lysates. For each drug concentration, cell viability was determined after 24 hrs using Cell Titer Glo assay (b, d, f). Values are expressed as a percentage of control condition that was taken as 100%. A representative experiment is shown. Values are means of triplicates ± SEM. p-values are calculated by comparing each treated-condition with the mock.

Figure 2: Cholesterol transport inhibitors regulate intracellular CHIKV replication

(A) Post-infection addition of lovastatin, U18666A or imipramine reduces CHIKV replication. Increasing concentrations of drugs were added to HEK293T cells 1 hr after CHIKV infection at a MOI of 1. After 24 hrs, CHIKV replication was monitored by quantification of GFP fluorescence in the cell lysates. Values, normalized to the protein content in the samples, are expressed as a percentage of the non-infected (NI) condition. (B) Schematics of CMV-P1234 and HSPolI-Fluc-Gluc constructs, plasmid backbones are shown. (C) HEK293T cells were transfected with plasmids depicted in (B) and treated with the indicated concentrations of lovastatin, U18666A or imipramine at 2 hrs post-transfection. Firefly and Gaussia luciferase activities were determined after 24 hrs in culture. A representative experiment is shown. Values are expressed as a percentage of the untreated condition and are means of triplicates ± SEM. NT designates non-transfected control cells. p-values are calculated by comparing each treated-condition with the mock.

Figure 3: CHIKV nsP1 associates with the PM through conserved sequence motifs

(A) Organization of the CHIKV nsP1. Conserved amino-acids involved in the central α-helix (aa 244-263) and those required for nsP1 acylation (417-419) are indicated. Mutants used in this study are depicted. (B) Membrane affinity of GFP-nP1, GFP-nsP1$_{3A}$, GFP-nsP1$_{W258A}$ and GFP-nsP1$_{DM}$ was determined by cell fractionation assays. HEK293T cells transfected to express each GFP-fused protein were fractionated to produce cytosolic (S25) and membranous (P25) fractions. Equal amounts of fractions were analyzed by SDS-PAGE and western blotting with anti-nsP1 or anti-GFP antibodies. Antibodies against Na^+/K^+ ATPase (ATPase) and GAPDH were used to control the separation of membranes and cytosolic compartments respectively. For each experiment a sample of the unfractionated cell lysate (CL) was run in parallel to determine the relative amount of each nsP1 mutant expressed. Cells expressing the GFP protein alone are shown as a control. (C) The intensity of bands in S25 and P25 samples from panel B was determined using Image J software and plotted as a histogram. (D) Subcellular localization of GFP-nsP1 and its mutant was determined by confocal imaging of transfected HeLa cells. Cell membranes are labeled with Alexa Fluor 647-conjugated wheat germ hemagglutinin (WGA). Scale bars are 5 μm. (E) Confocal microscopy imaging of HeLa cells transfected with expression plasmids for nsP1-GFP or for an untagged nsP1. The untagged nsP1 protein was detected with rabbit antiserum and Alexa-647-conjugated secondary reagents. Nuclei were stained with DAPI before analysis by confocal imaging. GFP-nsP1 at the plasma membrane and filopodia-like structures formed at the surface of transfected cells are indicated by white arrows. Cytosolic aggregates are indicated by blue arrows. Bars: 5 μm. (F) Lysates of cells expressing GFP-nP1, GFP-nsP1$_{3A}$, GFP-nsP1$_{W258A}$, GFP were subjected to membrane flotation assay in iodixanol gradient. Fractions collected from top to bottom were separated on SDS-PAGE and probed with antibodies specific for nsP1. Lysates from GFP expressing cells were probed with antibodies specific for GFP, flotillin-1 (FLOT1) or ATPase. Data are representative of three separate experiments.

Figure 4: Cholesterol trafficking inhibitors redirect nsP1 to endo/lysosomal compartments

(A) HeLa cells cultured in the presence of 12 μM U18666A were stained with filipin III to visualize cholesterol distribution. Cells cultured in medium containing an appropriate amount of vehicle are

836 shown as control (Mock). (B) Cells expressing the GFP-nsP1 protein were maintained for 24 hrs in the
837 presence of 12 μM U18666A and then co-labeled with filipin III and anti-Lamp2 antibodies to
838 visualize cholesterol and endo/lysosomes respectively. Cells maintained with vehicle alone are
839 shown as controls (Mock). (C) Consequences of U18666A treatment on GFP-nsP1 membrane binding
840 capacity was determined by cell fractionation assays. Crude lysates (CL) and cytosolic fractions (S25)
841 prepared from mock-treated or U18666A-treated HEK293T cells were separated on SDS-PAGE and
842 probed with antibodies against GFP or GAPDH. (D) HeLa cells transfected with GFP or GFP-nsP1
843 expression plasmid and maintained with 12 μM U18666A or in medium alone (Mock) for 24 hrs were
844 stained with filipin III and DAPI and then processed for confocal imaging. (E) Histograms indicate the
845 signal intensity profile of filipin III and green fluorescence along the white lines in (D). Bars: 5 μm. (F)
846 Colocalization of filipin and GFP signals in U18666A-treated cells was determined by calculation of
847 Mander's overlap coefficients (n ≥ 20 cells).

848 **Figure 5: GFP-nsP1$_{W258A}$ and GFP-nsP1$_{3A}$ display different sensitivity to U18666A-induced**
849 **cholesterol storage defect.**
850 HeLa cells expressing either GFP-nsP1$_{3A}$ (A) or GFP-nsP1$_{W258A}$ (C) were incubated with 12 μM
851 U18666A for 24 hrs. Unesterified cholesterol was stained with filipin-III and cells were processed for
852 confocal microscopy. (B) and (D) Histograms showing filipin III and GFP fluorescence intensity along
853 the white lines indicated in (A) and (B) respectively. Bars: 5 μm. (E) Colocalization of filipin and GFP
854 signals in U18666A-treated cells was determined by calculation of Mander's overlap coefficients (n ≥
855 20 cells).

856 **Figure 6: C417-419 are key determinants for CHIKV nsP1 targeting to CD81-positive cholesterol-rich**
857 **compartments**
858 U2OS cells expressing (A) the GFP, (B) GFP-nsP1, (C) GFP-nsP1$_{3A}$ were cultured in control condition or
859 in medium supplemented with 12 μM U18666A or 75 μM imipramine for 24 hrs. Then, the cells were
860 probed with anti-CD81 mAbs and Alexa Fluor-594-conjugated secondary antibodies. Nuclei were

stained with DAPI and the cells were processed for confocal microscopy. Scale bars are 5 μm. (D) Quantification of the degrees of colocalization of GFP fluorescence and CD81 staining in treated cells was determined by calculation of Mander's and Pearson's overlap coefficients (n ≥ 20 cells). (E and F) 3D image reconstruction was performed from z-stacks acquired from treated cells expressing either GFP-nsP1 or GFP-nsP1$_{3A}$.

Figure 7: CHIKV nsP1 partitioning with lipid rafts in human cells requires C417-419

(A) HEK293T cells were transfected with plasmids encoding GFP-nsP1 and processed for raft isolation. Nine fractions of the density gradients, numbered from top to bottom, were collected and analyzed using SDS-PAGE. Proteins were probed with antibodies against nsP1, FLOT1 and Na+/K+ ATPase. Fractions containing detergent-resistant membranes (DRMs) and detergent soluble membranes (DS) are indicated. (B) The amount of GFP-nsP1 and FLOT1 associated with each fraction was determined by densitometry scanning of immunoblots and expressed as a percentage of total protein expression level. The diagram is representative of three experiments. (C, D) A similar experiment was performed starting from cells incubated for 30 minutes in the presence of 10 mM βMCD**.** (E) Cells expressing the GFP-nsP1$_{3A}$ or GFP-nsP1$_{W258A}$ mutants were processed as in (A). (F) Amounts of GFP-nsP1, GFP-nsP1$_{3A}$ or GFP-nsP1$_{W258A}$ in DRM and DS fractions were determined by densitometry scanning of the immunoblots shown in (A) and (E) and expressed as a percentage of total protein signal.

Figure 8: nsPs expressed by a CHIKV trans-replicase or an infectious CHIKV co-segregate with DRMs depending of nsP1 C417-419. DRMs were isolated from (A) HEK293T cells transfected with CMV-P1234 and HSPolI-Fluc-Gluc plasmids (depicted in Fig 2B); (B) cells infected with CHIKV-LR-5'GFP (MOI 0.1); (C) cells transfected with CMV-P1$_{3A}$234 and HSPolI-Fluc-Gluc plasmids. After 24 hrs, fractions were prepared and analyzed as described for Fig 7A, immunoblots were probed with antibodies against each CHIKV nonstructural protein as indicated. (D and E) Amounts of nsPs in DRM

885 and DS fractions were determined by densitometry scanning of the immunoblots shown in (A) and
886 (B) respectively and expressed as a percentage of total protein signal.

887 **Figure 9: SINV nsP1 affinity for cholesterol.** (A) Organization of the SINV nsP1 and mutant studied.
888 Conserved amino-acids involved in the central α-helix (aa 245-264) and palmitoylated cysteine (C420)
889 are indicated. Mutant used in this study is depicted. (B) HEK293T cells transfected with either SINV
890 GFP-nsP1 or GFP-nsP1$_{C420A}$ plasmids were processed for DRMs isolation as described for Fig 7.
891 Fractions (numbered from top to bottom) were probed in immunoblot with antibodies against GFP.
892 (C) HeLa cells were transfected with a plasmid encoding a SINV GFP-nsP1 protein for 4 hrs and
893 cultured for an additional 24 hrs in the presence of 12 μM U18666A. Cells were labeled with filipin III
894 to visualize cholesterol. Controls cells (Mock) were maintained with vehicle. (D) HeLa cells
895 transfected to express the GFP-nsP1$_{C420A}$ mutant were processed as in (C). Bars: 5 μm.

896 **Figure 10: Model for nsP1/cholesterol interplay in transfected and CHIKV-infected cells.** a)
897 Palmitoylated cysteines in wild type nsP1 are critical for targeting to cholesterol-rich membranes
898 microdomains. In infected cells, the preferential association of nsP1 with DRMs increases its local
899 concentration which may facilitate its oligomerization and dictates the localization of a fraction of
900 other nsPs to lipid rafts. In this scenario CHIKV efficiently replicates its genome. b) Imipramine and
901 U18666A, by inhibiting cholesterol trafficking to the PM, generate nsP1 accumulation in Lamp2-
902 positive late endosomes/lysosomes. Association of nsP2, nsP3 and nsP4 to cholesterol rich
903 microdomains is no more observed. Under these conditions, CHIKV genome replication is abolished
904 by a mechanism that remains to be fully elucidated. c) nsP1$_{3A}$ that weakly interacts with the plasma
905 membrane is not targeted to DRMs. In this situation CHIKV genomes replication is impaired. For
906 simplicity, only mature nsPs are shown in this model. In natural infection, the membrane association
907 begins by modification and membrane targeting of polyprotein precursors.

A

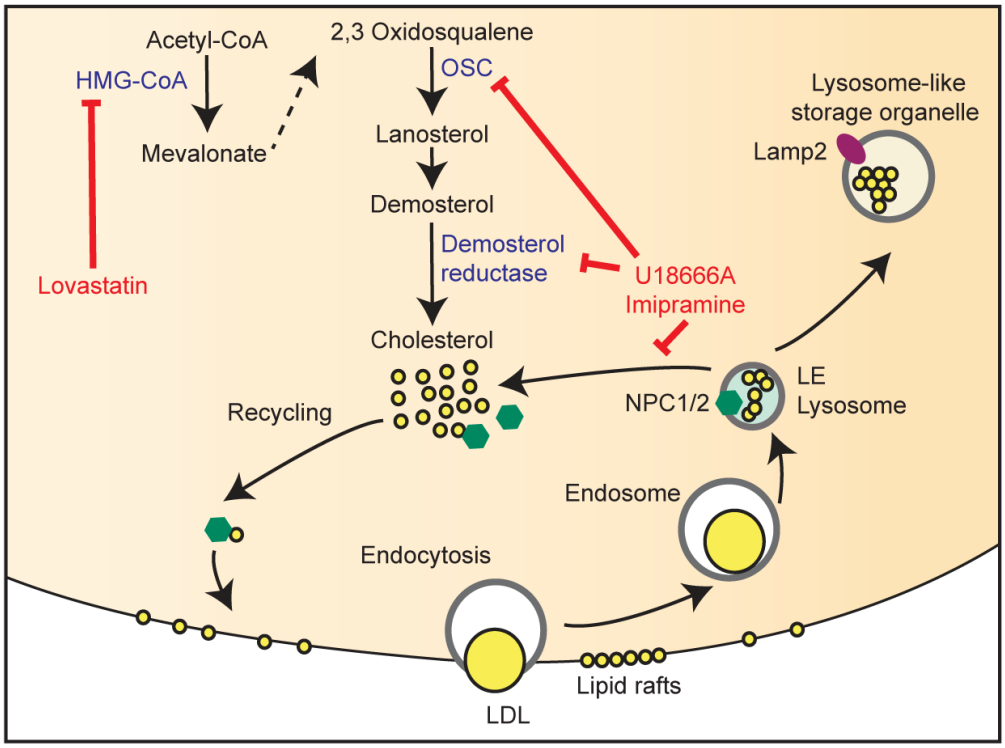
Acetyl-CoA
2,3 Oxidosqualene
HMG-CoA
OSC
Lysosome-like
storage organelle
Mevalonate
Lanosterol
Lamp2
Demosterol
Demosterol
reductase
U18666A
Imipramine
Lovastatin
Cholesterol
LE
Lysosome
NPC1/2
Recycling
Endosome
Endocytosis
Lipid rafts
LDL

B

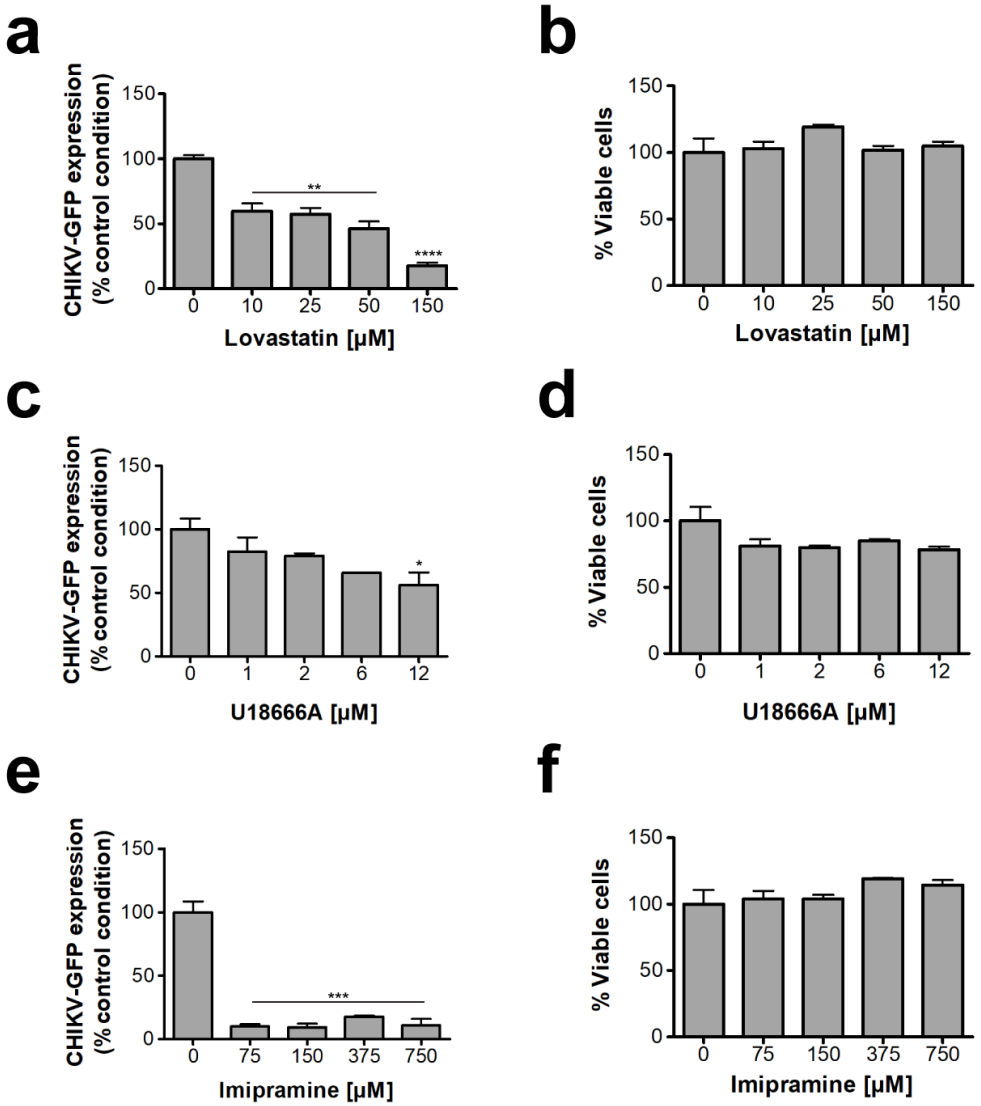
a
CHIKV-GFP expression
(% control condition)
150
100
50
0
**
****
0
10
25
50
150
Lovastatin [μM]
b
% Viable cells
150
100
50
0
0
10
25
50
150
Lovastatin [μM]
c
CHIKV-GFP expression
(% control condition)
150
100
50
0
*
0
1
2
6
12
U18666A [μM]
d
% Viable cells
150
100
50
0
0
1
2
6
12
U18666A [μM]
e
CHIKV-GFP expression
(% control condition)
150
100
50
0
***
0
75
150
375
750
Imipramine [μM]
f
% Viable cells
150
100
50
0
0
75
150
375
750
Imipramine [μM]

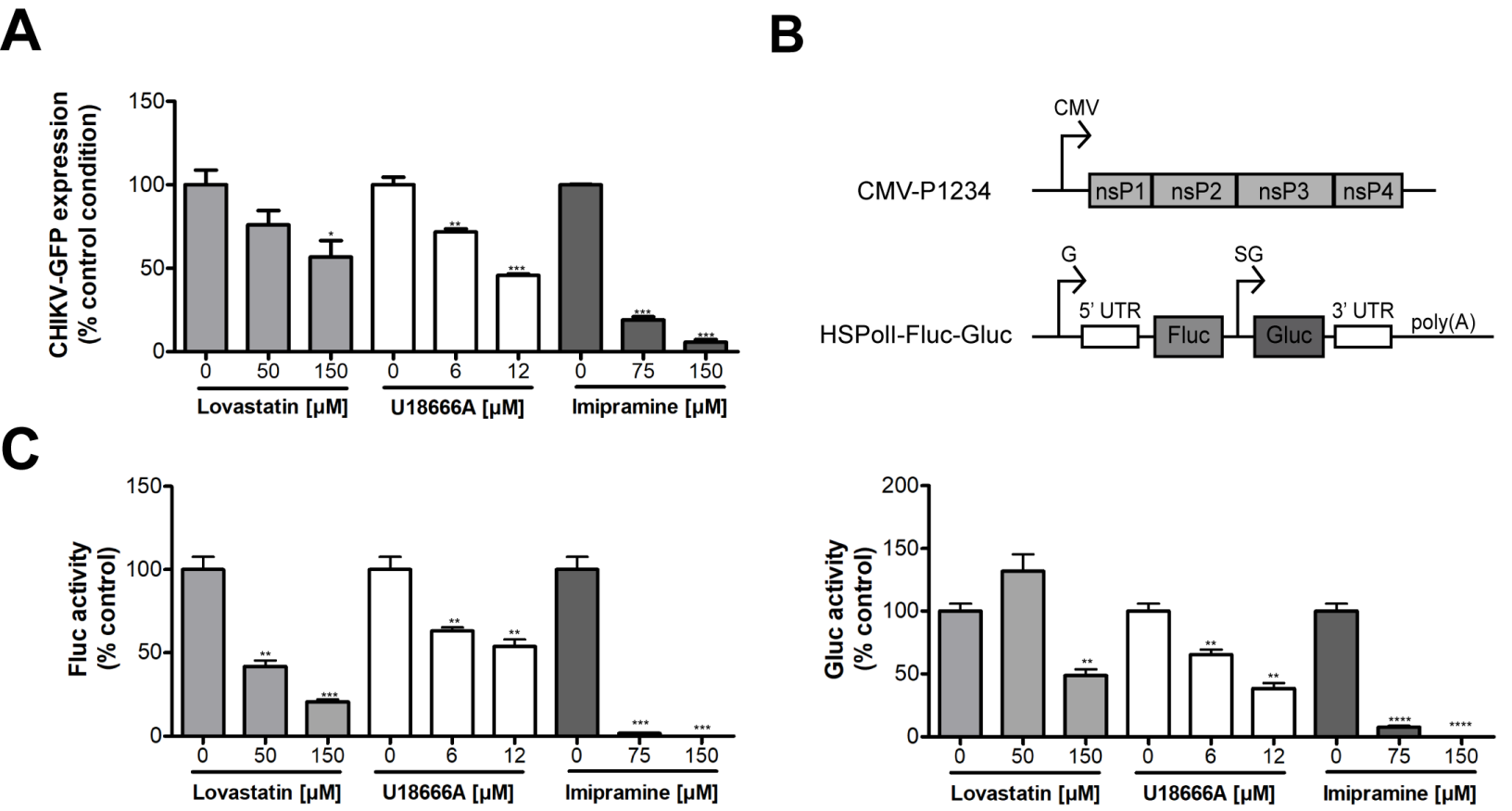
A
CHIKV-GFP expression (% control condition)
150
100
50
0
0 50 150 0 6 12 0 75 150
Lovastatin [μM]
U18666A [μM]
Imipramine [μM]
B
CMV
CMV-P1234
nsP1
nsP2
nsP3
nsP4
G
SG
HSPolI-Fluc-Gluc
5' UTR
Fluc
Gluc
3' UTR
poly(A)
C
Fluc activity (% control)
Gluc activity (% control)
200
150
100
50
0
0 50 150 0 6 12 0 75 150
Lovastatin [μM]
U18666A [μM]
Imipramine [μM]

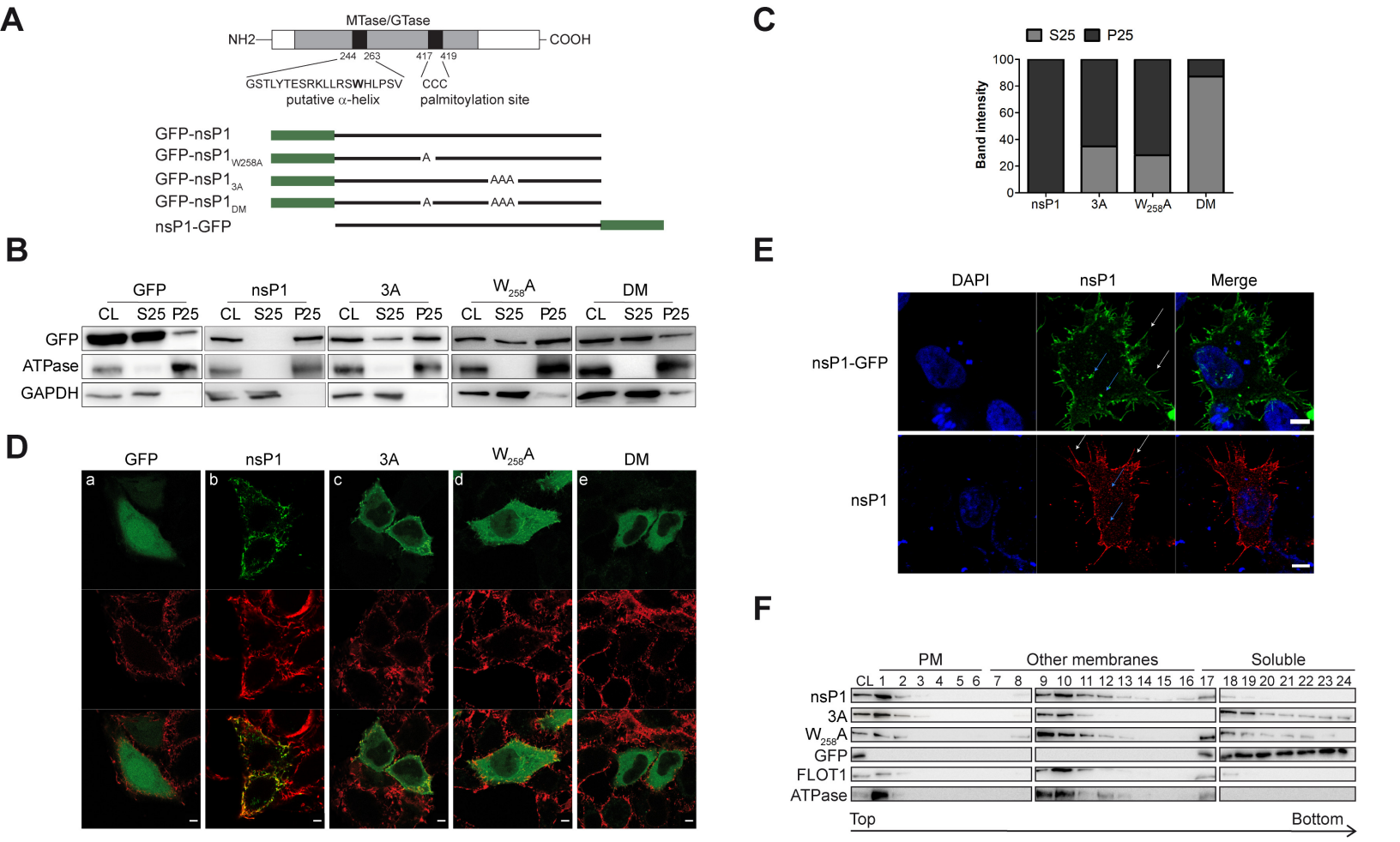
A
MTase/GTase
NH2
COOH
244 263 417 419
GSTLYTESRKLLRSWHLPSV
CCC
putative α-helix
palmitoylation site
GFP-nsP1
GFP-nsP1W258A
GFP-nsP1 3A
GFP-nsP1DM
nsP1-GFP
A
AAA
A
AAA
B
GFP
nsP1
3A
W258A
DM
CL S25 P25
GFP
ATPase
GAPDH
C
S25 P25
Band intensity
100
80
60
40
20
0
nsP1
3A
W258A
DM
D
GFP
nsP1
3A
W258A
DM
a
b
c
d
e
E
DAPI
nsP1
Merge
nsP1-GFP
nsP1
F
PM
Other membranes
Soluble
CL 1 2 3 4 5 6 7 8 9 10 11 12 13 14 15 16 17 18 19 20 21 22 23 24
nsP1
3A
W258A
GFP
FLOT1
ATPase
Top
Bottom

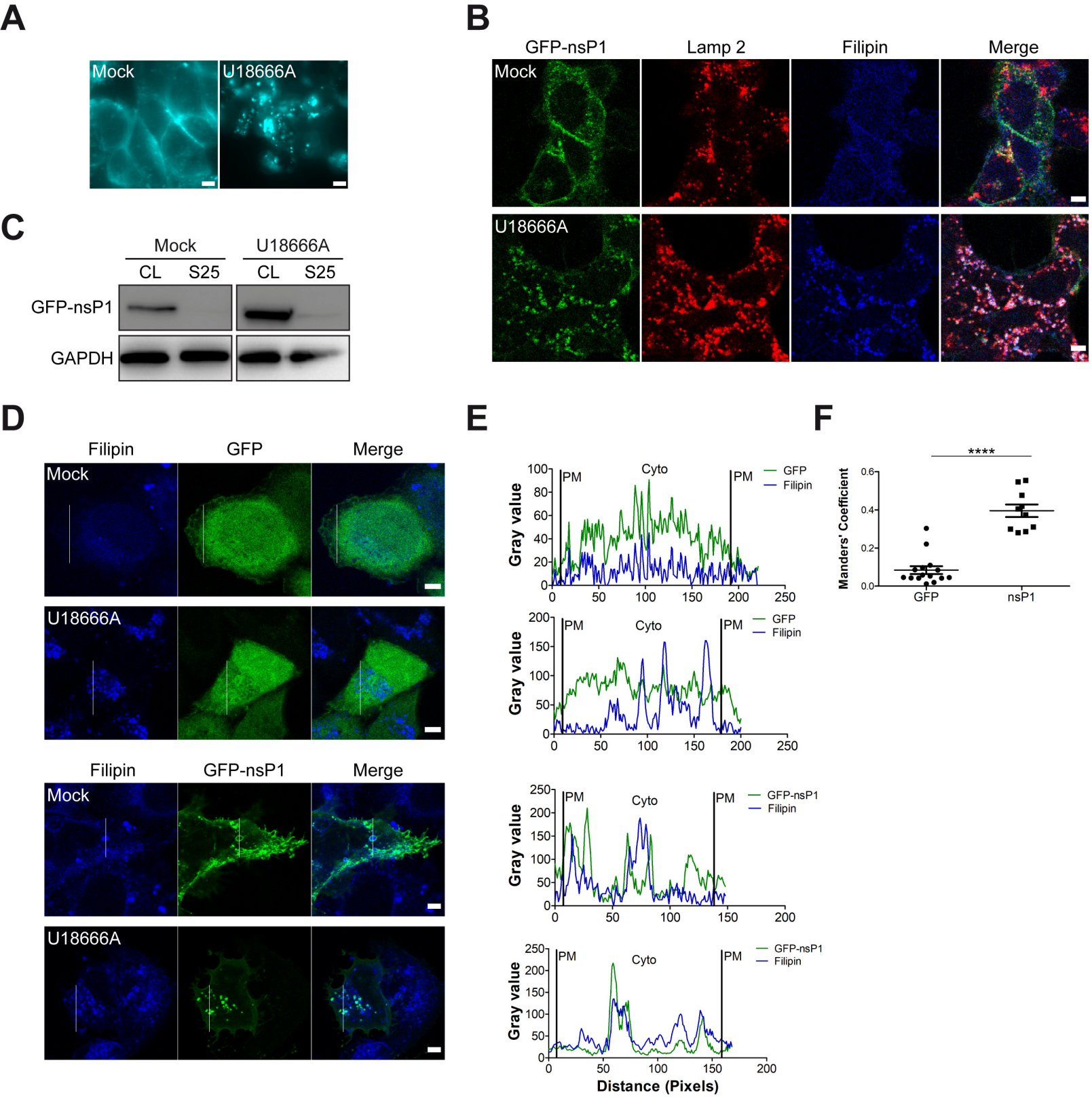
A
Mock
U18666A
B
GFP-nsP1
Lamp 2
Filipin
Merge
Mock
U18666A
C
Mock
U18666A
CL
S25
CL
S25
GFP-nsP1
GAPDH
D
Filipin
GFP
Merge
Mock
U18666A
Filipin
GFP-nsP1
Merge
Mock
U18666A
E
PM
Cyto
PM
GFP
Filipin
Gray value
GFP-nsP1
Distance (Pixels)
F
****
Manders' Coefficient
GFP
nsP1

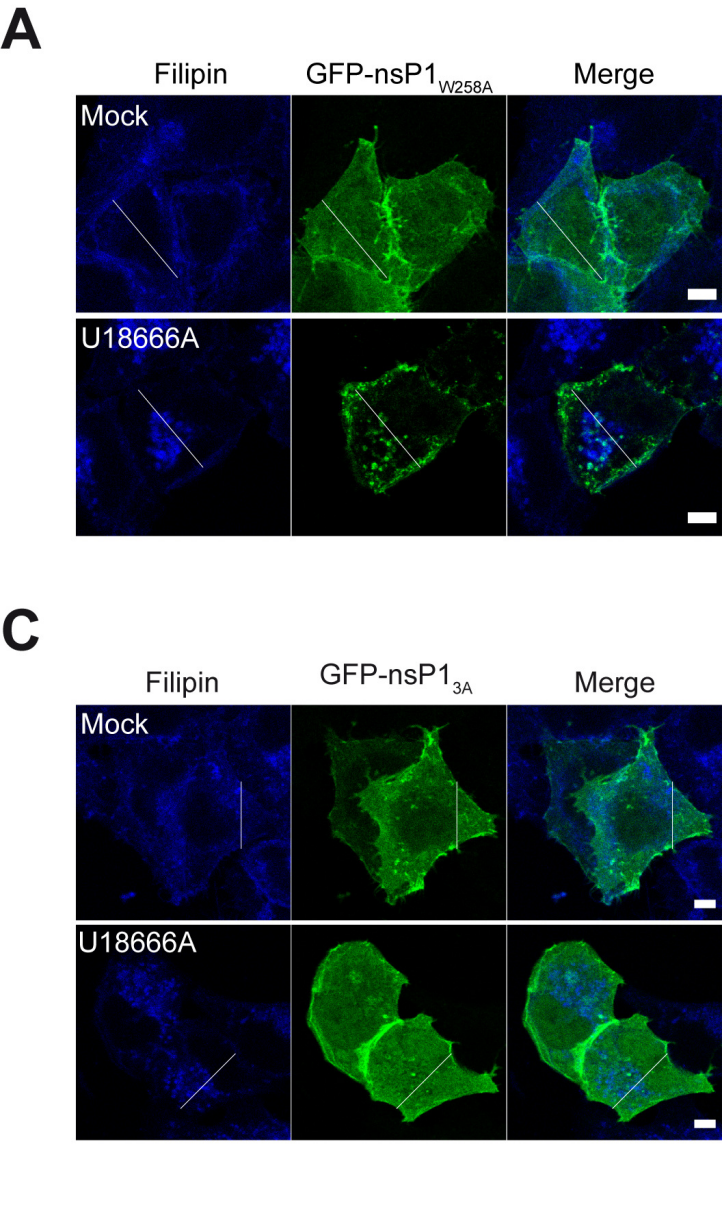
A
Filipin
GFP-nsP1W258A
Merge
Mock
U18666A
B
GFP-nsP1W258A
Filipin
PM
Cyto
PM
Gray value
Distance (Pixels)
E
Manders' Coefficient
*
3A
W258A
C
Filipin
GFP-nsP13A
Merge
Mock
U18666A
D
GFP-nsP13A
Filipin
PM
Cyto
PM
Gray value
Distance (Pixels)

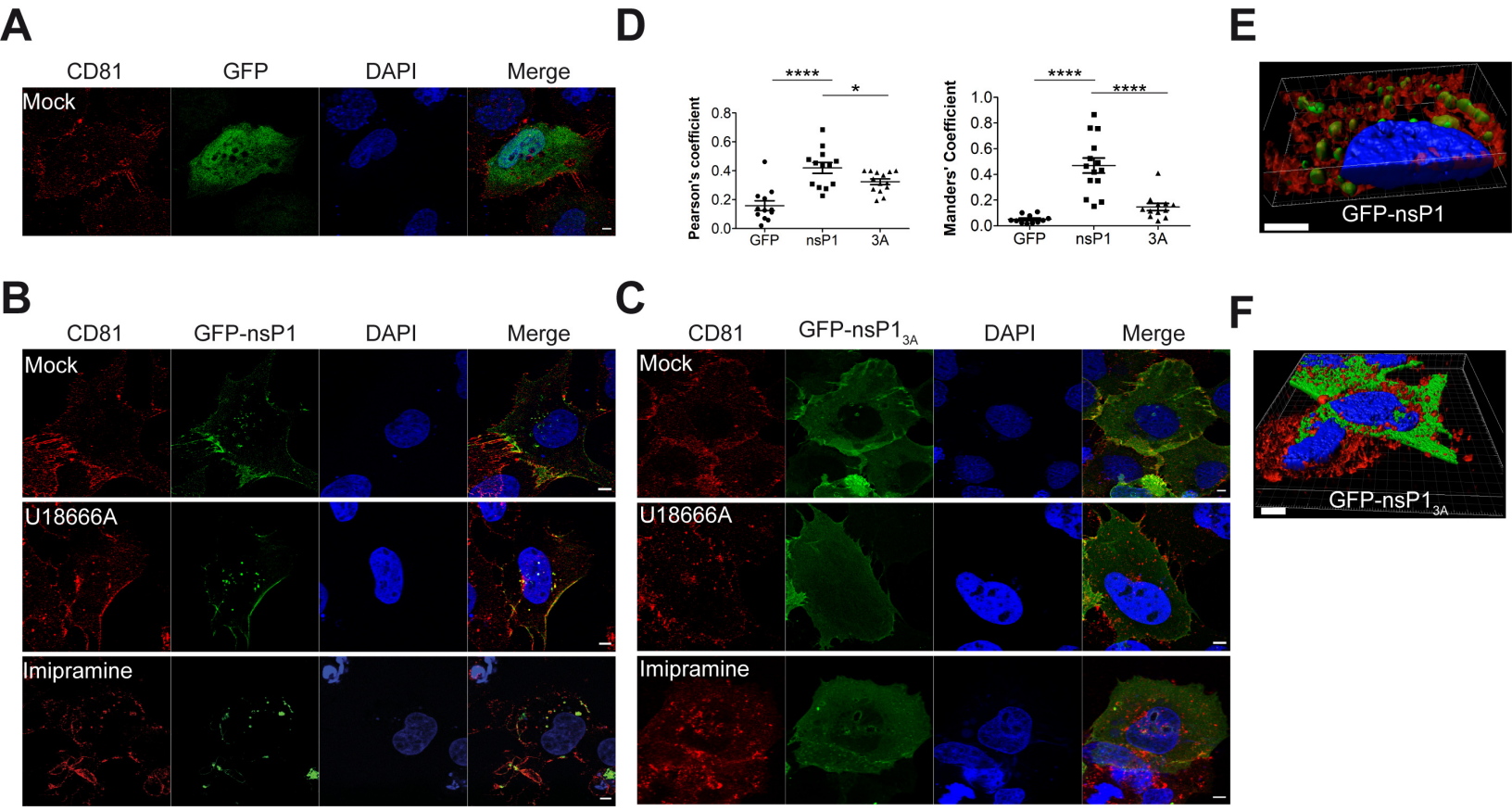
A
CD81
GFP
DAPI
Merge
Mock
B
CD81
GFP-nsP1
DAPI
Merge
Mock
U18666A
Imipramine
C
CD81
GFP-nsP1 3A
DAPI
Merge
Mock
U18666A
Imipramine
D
Pearson's coefficient
0.0
0.2
0.4
0.6
0.8
****
*
GFP
nsP1
3A
Manders' Coefficient
0.0
0.2
0.4
0.6
0.8
1.0
****
****
GFP
nsP1
3A
E
GFP-nsP1
F
GFP-nsP1 3A

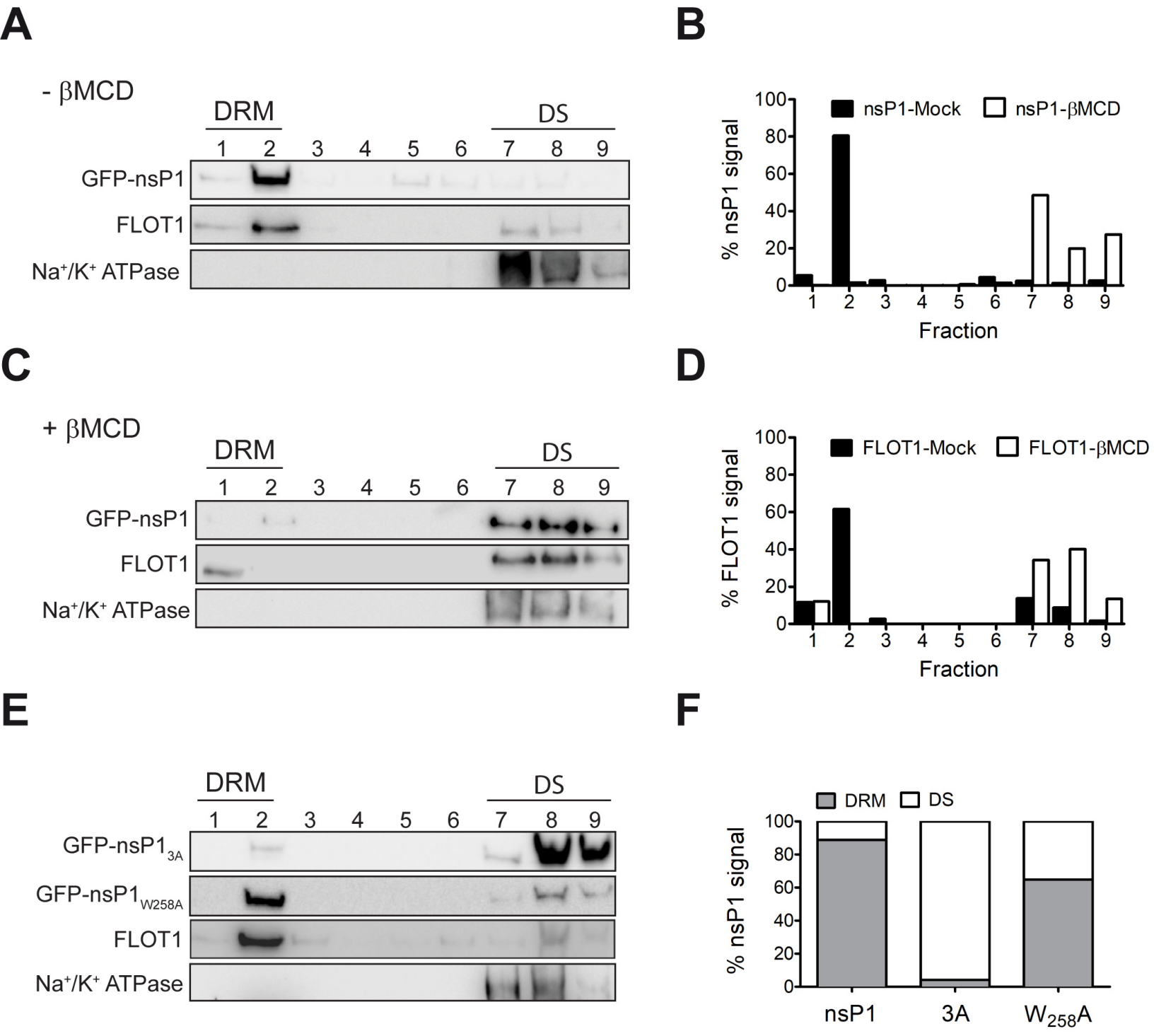
A
- βMCD
DRM
DS
1 2 3 4 5 6 7 8 9
GFP-nsP1
FLOT1
Na+/K+ ATPase
B
nsP1-Mock
nsP1-βMCD
% nsP1 signal
100
80
60
40
20
0
1 2 3 4 5 6 7 8 9
Fraction
C
+ βMCD
DRM
DS
1 2 3 4 5 6 7 8 9
GFP-nsP1
FLOT1
Na+/K+ ATPase
D
FLOT1-Mock
FLOT1-βMCD
% FLOT1 signal
100
80
60
40
20
0
1 2 3 4 5 6 7 8 9
Fraction
E
DRM
DS
1 2 3 4 5 6 7 8 9
GFP-nsP1 3A
GFP-nsP1 W258A
FLOT1
Na+/K+ ATPase
F
DRM
DS
% nsP1 signal
100
80
60
40
20
0
nsP1
3A
W258A

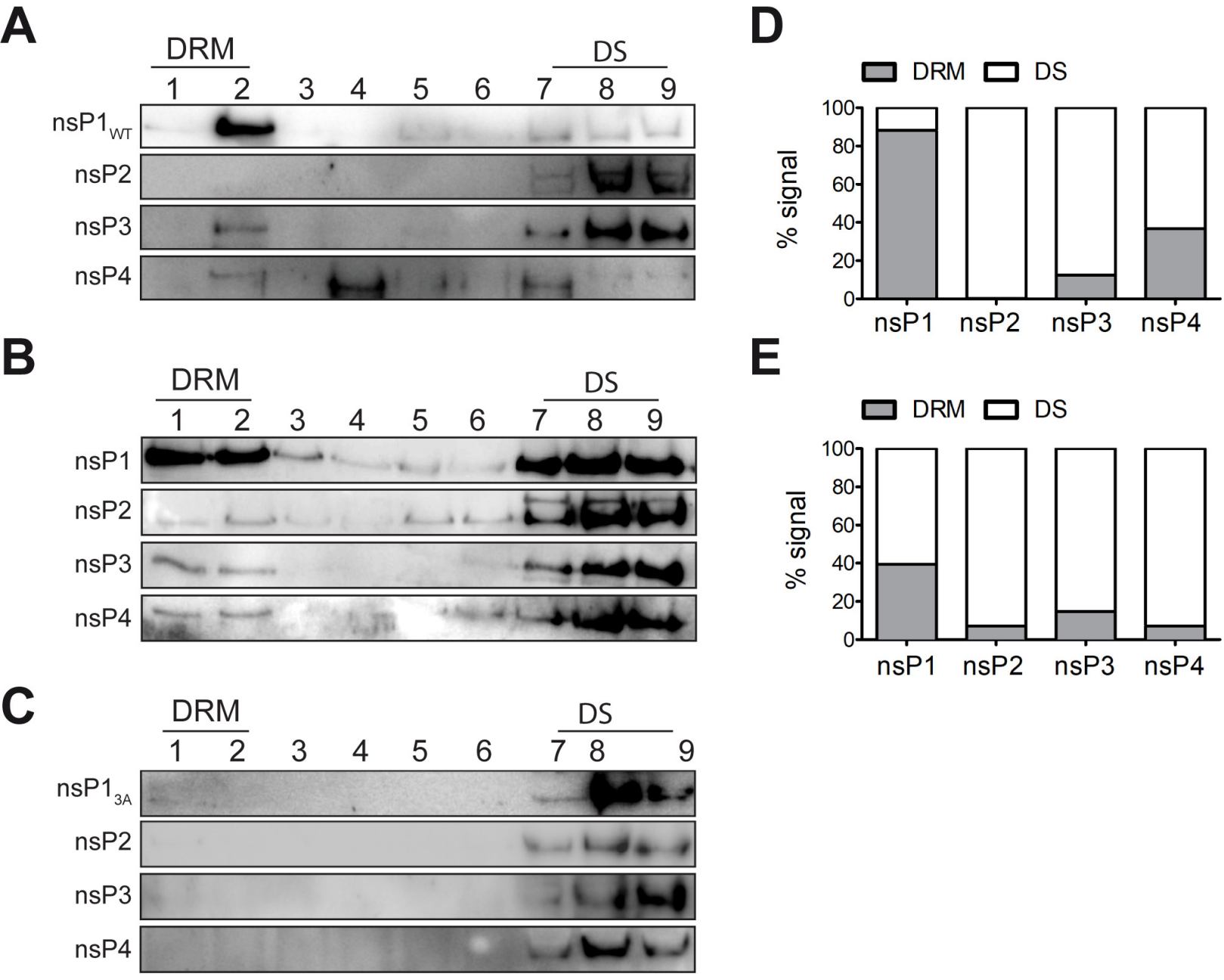
A
DRM
DS
1 2 3 4 5 6 7 8 9
nsP1WT
nsP2
nsP3
nsP4
B
DRM
DS
1 2 3 4 5 6 7 8 9
nsP1
nsP2
nsP3
nsP4
C
DRM
DS
1 2 3 4 5 6 7 8 9
nsP13A
nsP2
nsP3
nsP4
D
DRM
DS
% signal
100
80
60
40
20
0
nsP1
nsP2
nsP3
nsP4
E
DRM
DS
% signal
100
80
60
40
20
0
nsP1
nsP2
nsP3
nsP4

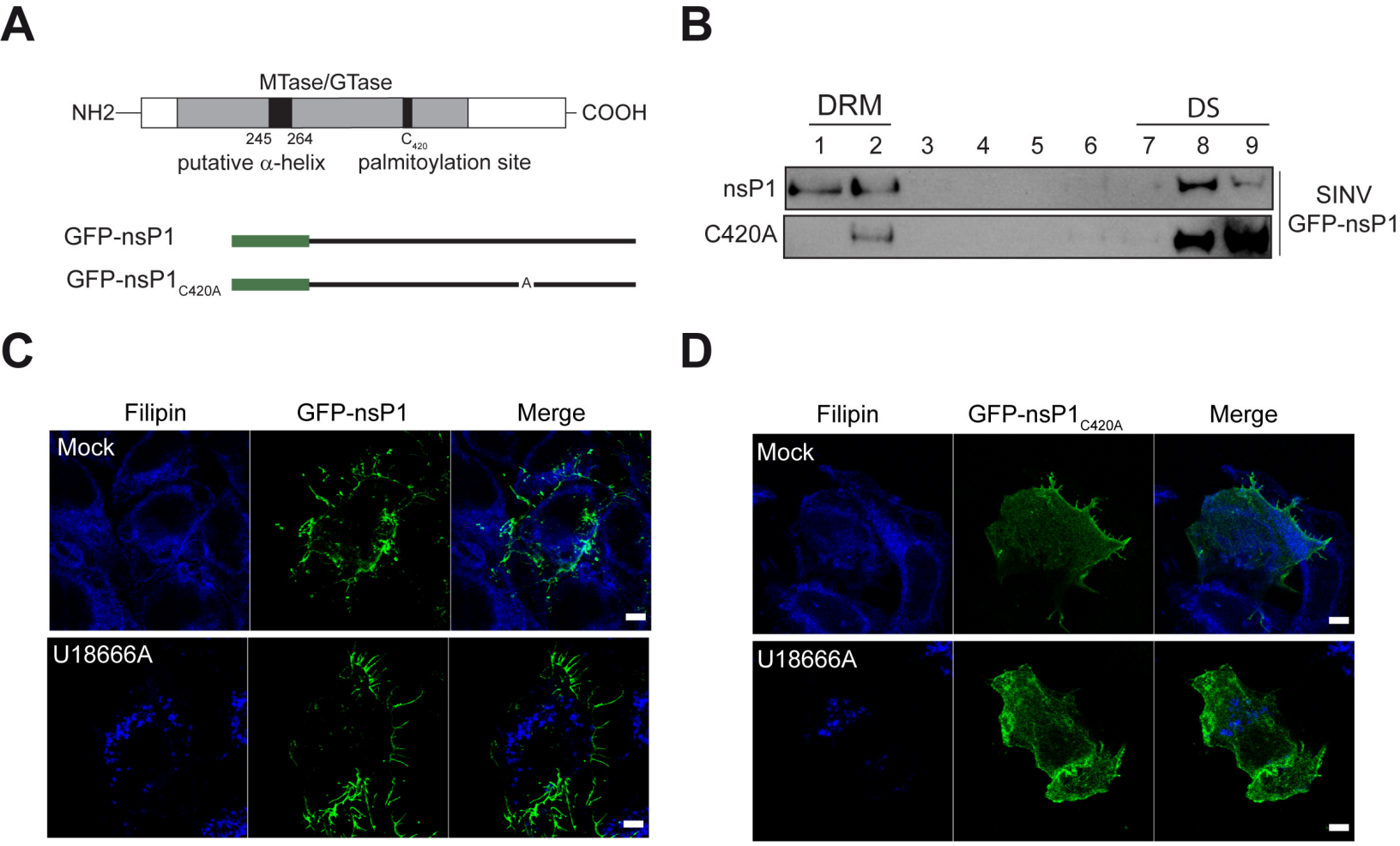
A
MTase/GTase
NH2
COOH
245
264
C420
putative α-helix
palmitoylation site
GFP-nsP1
GFP-nsP1C420A
A
B
DRM
DS
1
2
3
4
5
6
7
8
9
nsP1
C420A
SINV
GFP-nsP1
C
Filipin
GFP-nsP1
Merge
Mock
U18666A
D
Filipin
GFP-nsP1C420A
Merge
Mock
U18666A

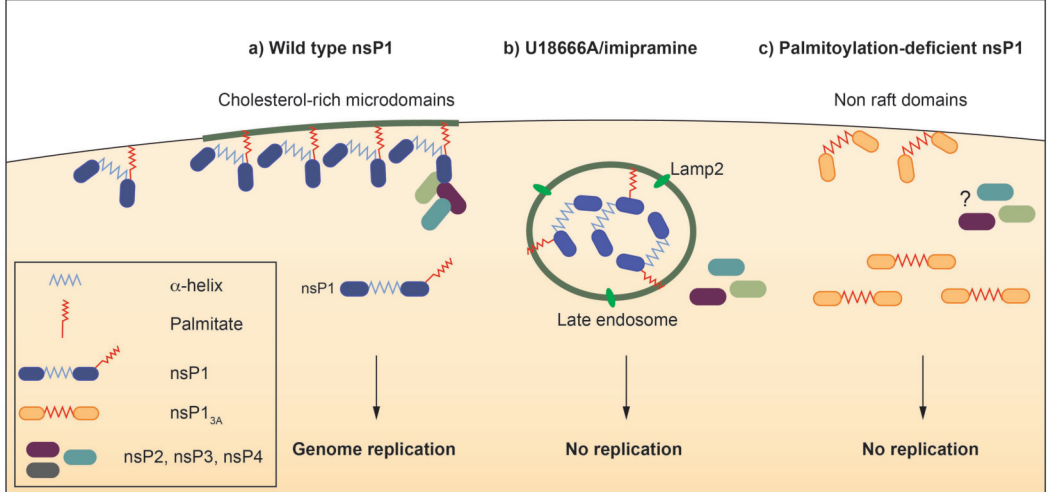
a) Wild type nsP1
b) U18666A/imipramine
c) Palmitoylation-deficient nsP1
Cholesterol-rich microdomains
Non raft domains
Lamp2
?
α-helix
Palmitate
nsP1
nsP1 3A
nsP2, nsP3, nsP4
nsP1
Late endosome
Genome replication
No replication
No replication